Biology 5357: Chemistry & Physics of Biomolecules
Fall 2023

Lecture 4: Membrane Dynamics

Janice L. Robertson
Dept. of Biochemistry & Molecular Biophysics
McDonnell Sciences Building 223A (Lab 223)
janice.robertson@wustl.edu

Lipid & membrane dynamics

Schematic representation of lipid motions in membranes [Charitat et al., 2008 adapted from Sackmann 1995].

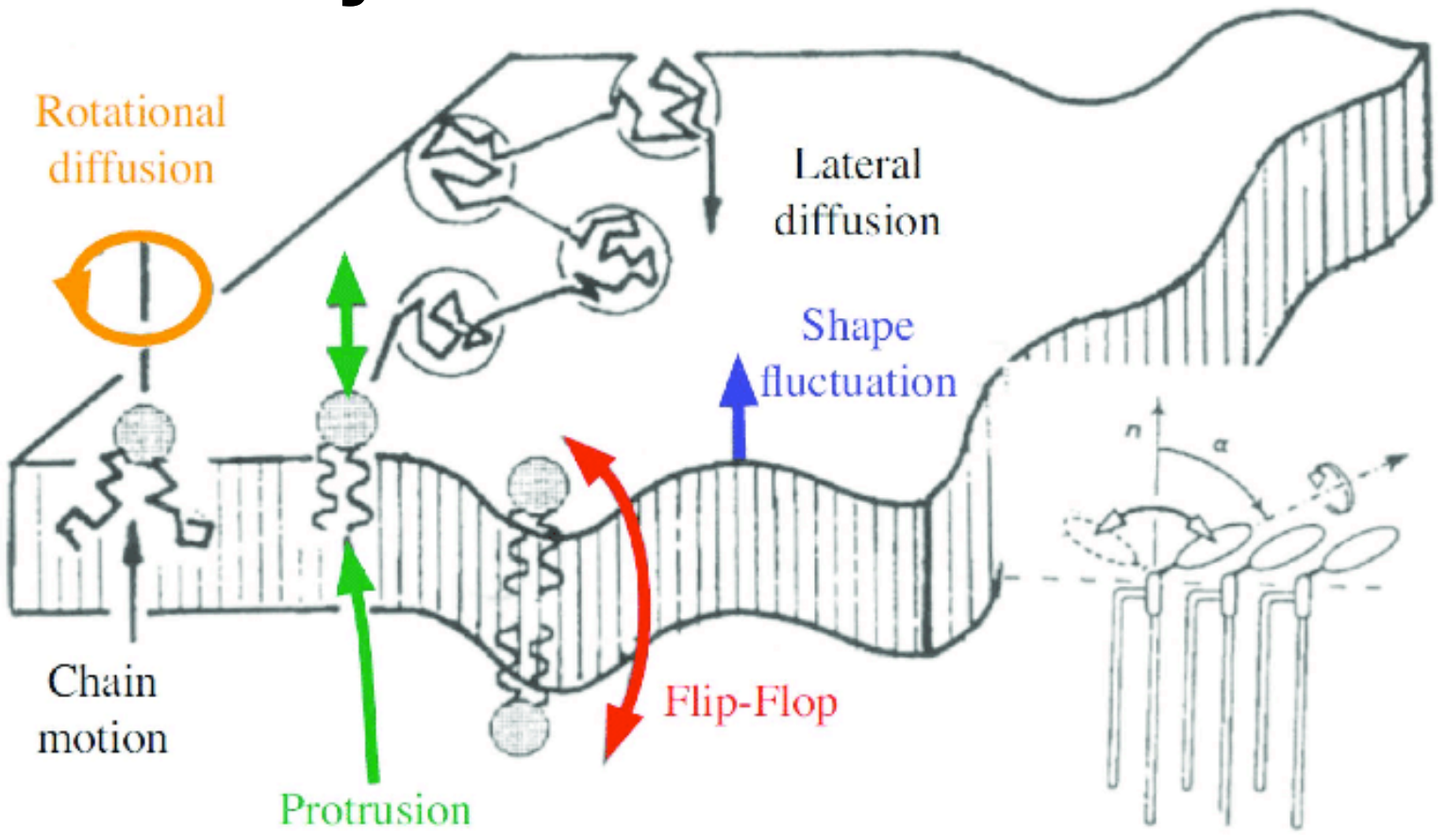

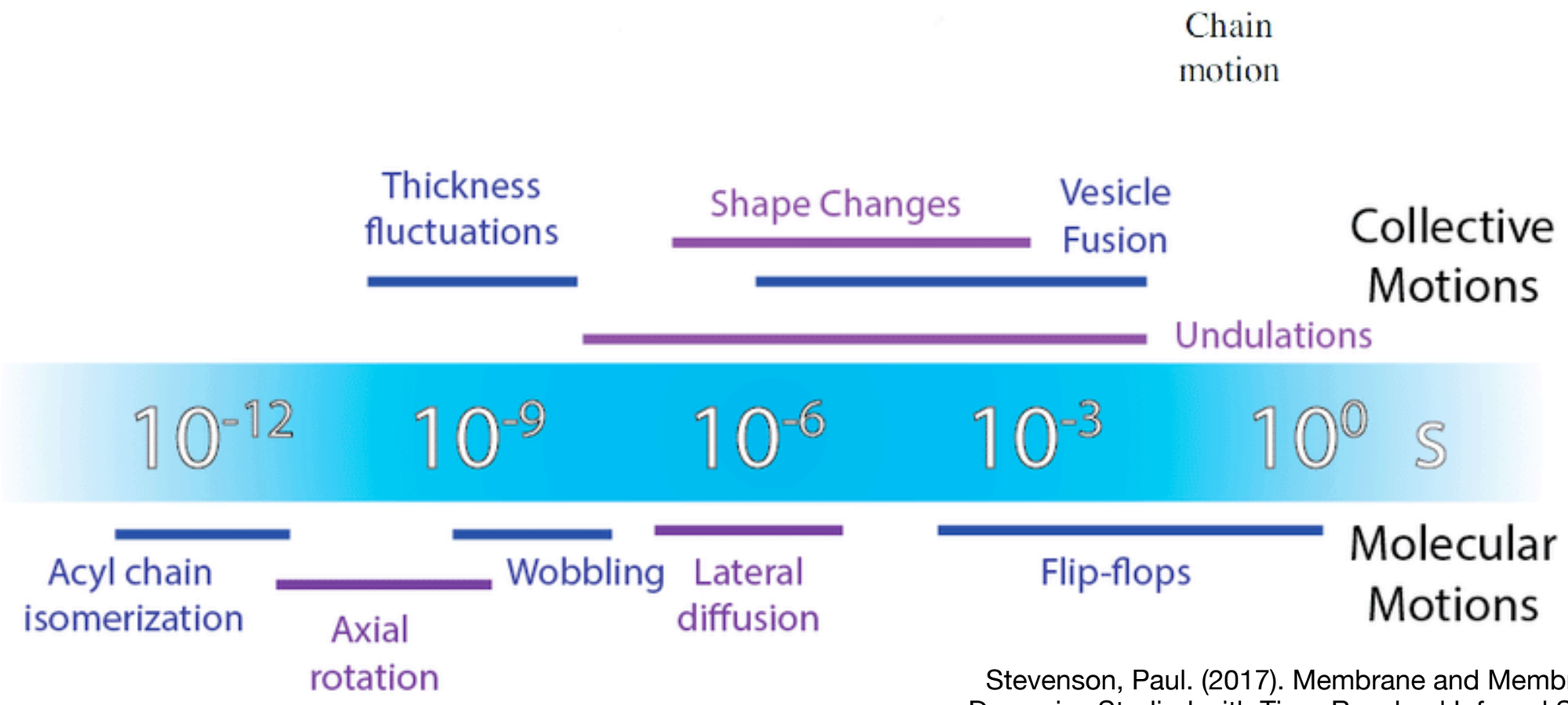

Stevenson, Paul. (2017). Membrane and Membrane Protein Dynamics Studied with Time-Resolved Infrared Spectroscopy.

Structures of lamellar phases

I.

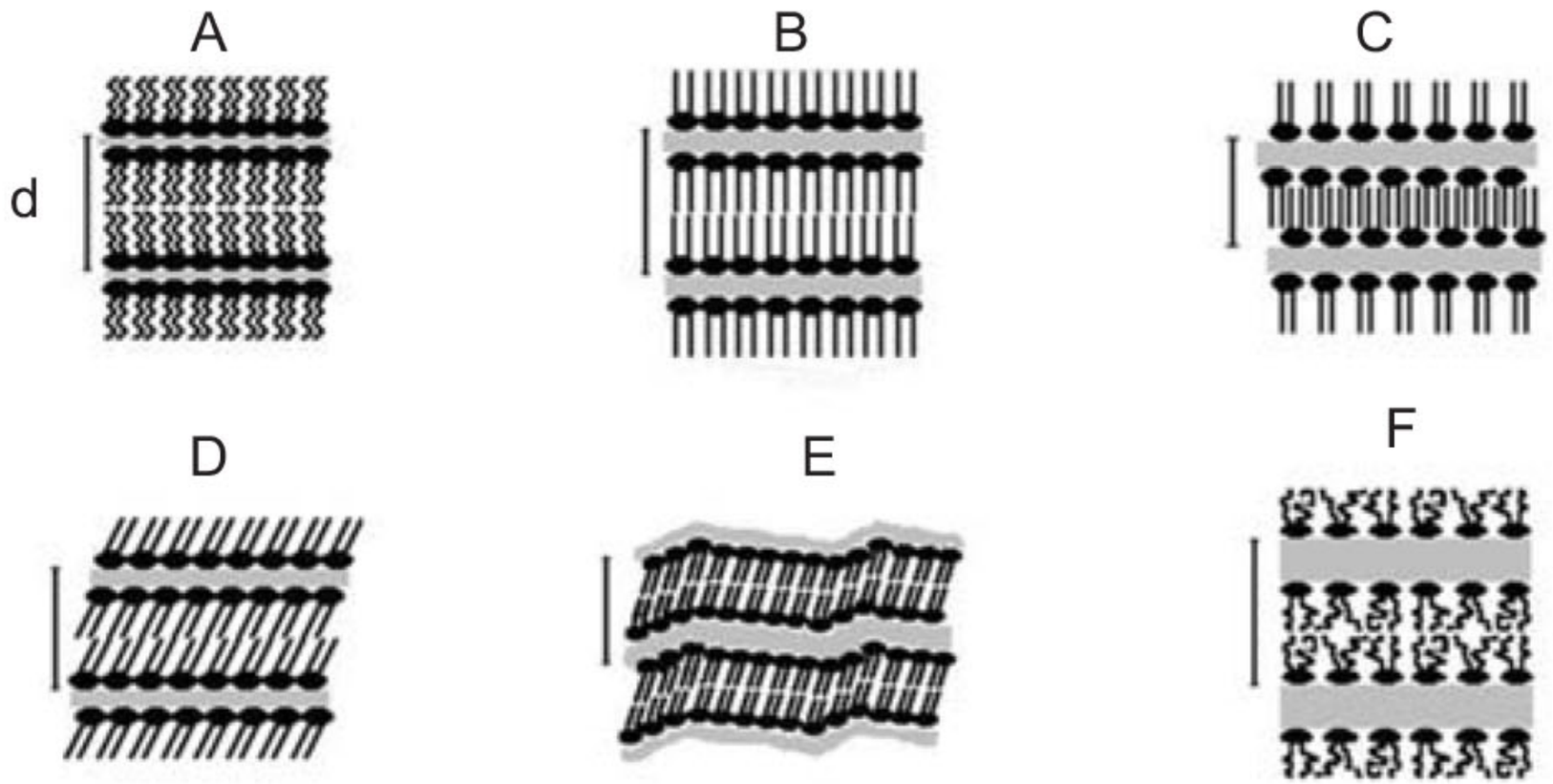

I. Lamellar phases: (A) subgel, L_c; (B) gel, L_β; (C) interdigitated gel, $L_\beta^{[int]}$; (D) gel, tilted chains, L_β'; (E) rippled gel, P_β'; (F) liquid crystalline, L_α . From Koynova R, Tenchov B. Transitions between lamellar and non-lamellar phases in membrane lipids and their physiological roles. OA Biochemistry 2013 Apr 01;1(1):9.

Lipid bilayer phase transitions

- Cooperative isomerization of trans to gauche configurations of acyl chains

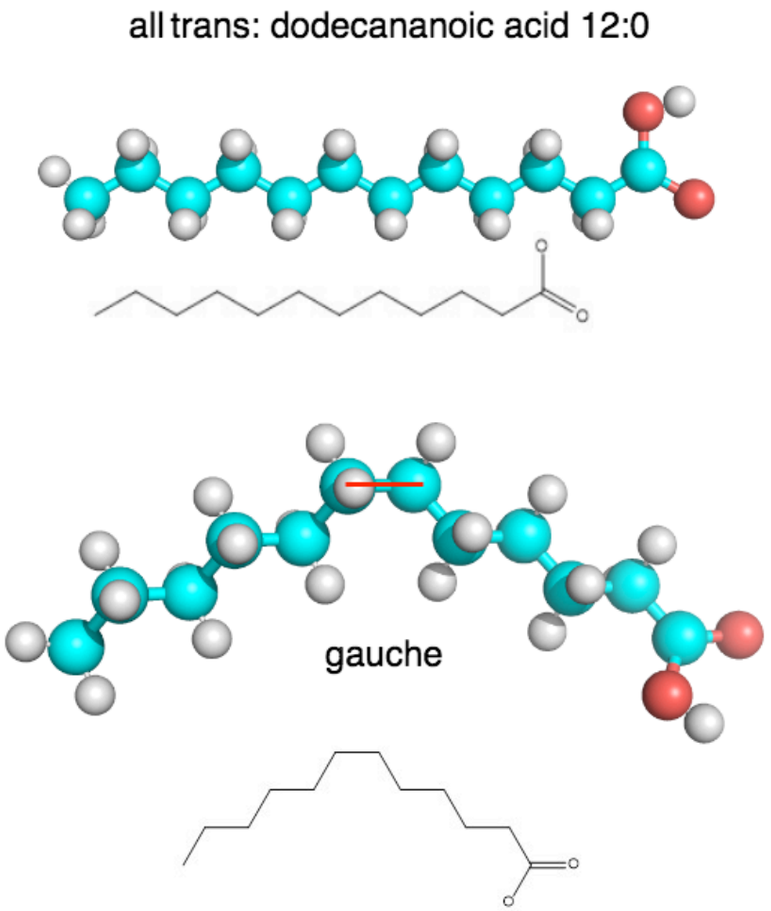

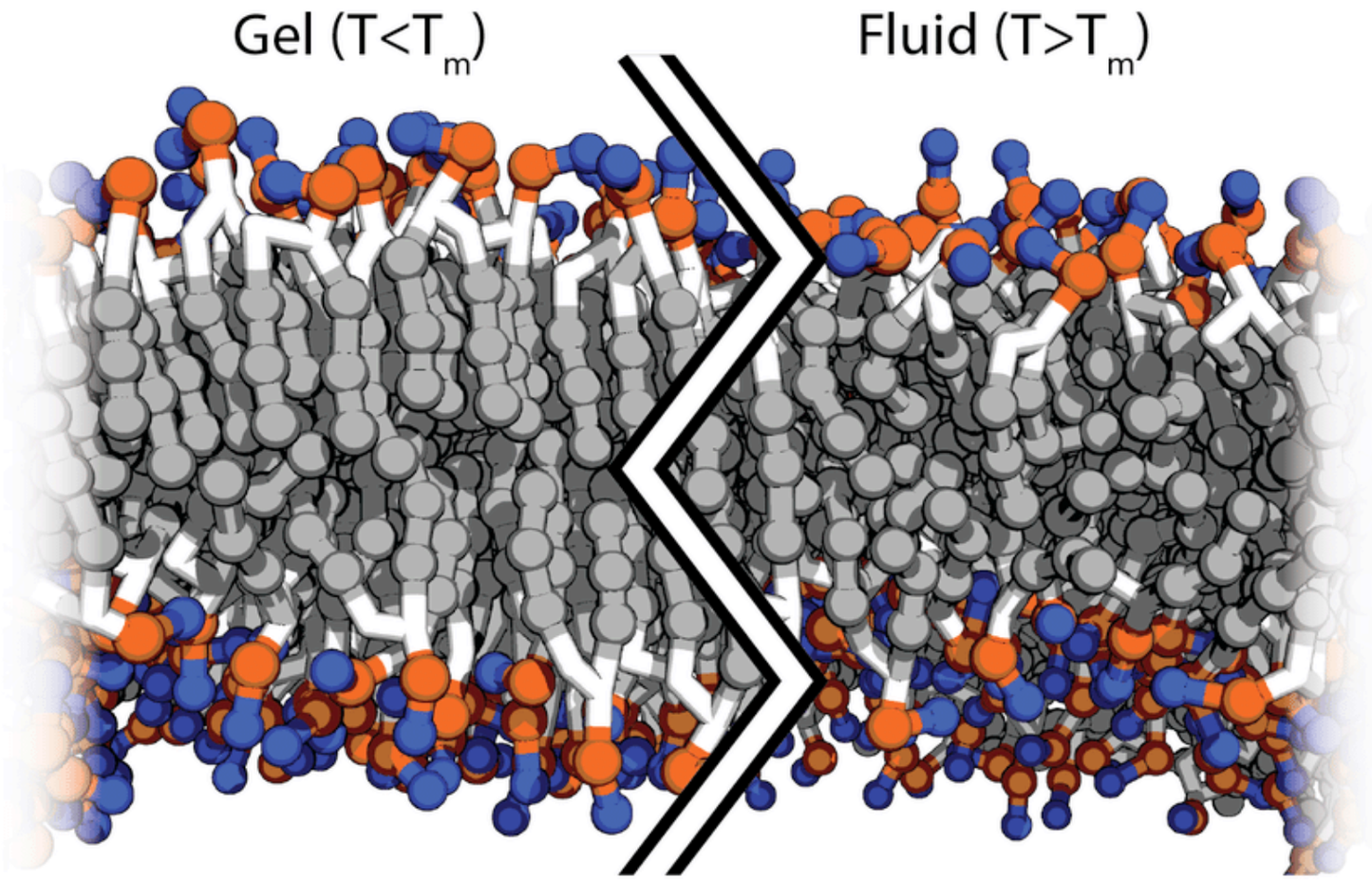

Stevenson, Paul. (2017). Membrane and Membrane Protein Dynamics Studied with Time-Resolved Infrared Spectroscopy.

Measuring membrane phase transitions - DSC

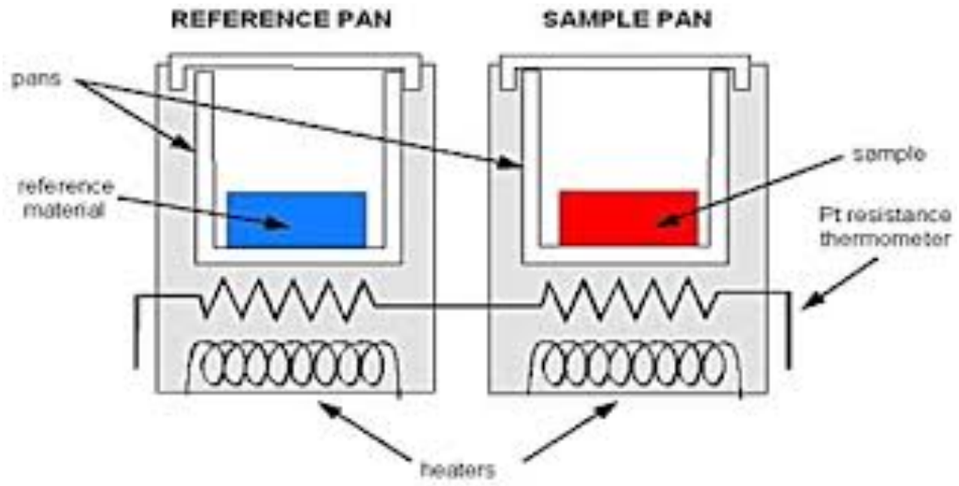

Differential Scanning Calorimetry (DSC) measures the difference in the amount of heat required to increase the temperature of a sample and reference cellar a function of T.

Heat flow = heat/time = q/t

Heating rate = temperature increase/time = ΔT/t

(q/t)/(ΔT/t) = q/ΔT = C_p = heat capacity

$$\Delta H = \int_{T_1}^{T_2} \left(\frac{\partial H}{\partial T}\right)_P dT = \int_{T_1}^{T_2} C_P \, dT$$

$$\Delta S = \frac{\Delta H_{cal}}{T_m}$$

Biomembrane models and drug-biomembrane interaction studies: Involvement in drug design and development.
Pignatello R, Musumeci T, Basile L, Carbone C, Puglisi G - J Pharm Bioallied Sci (2011)

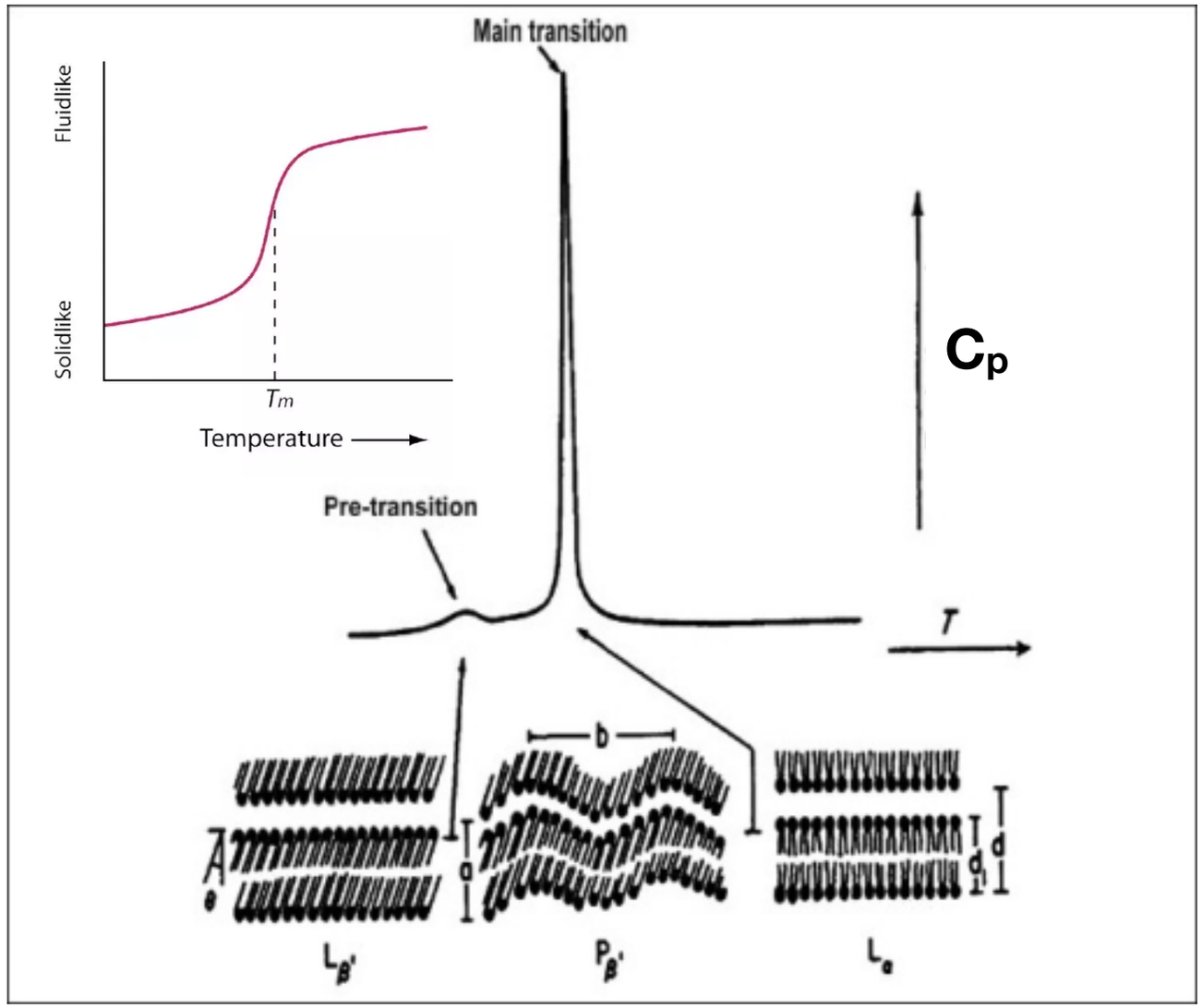

Atomic force microscopy

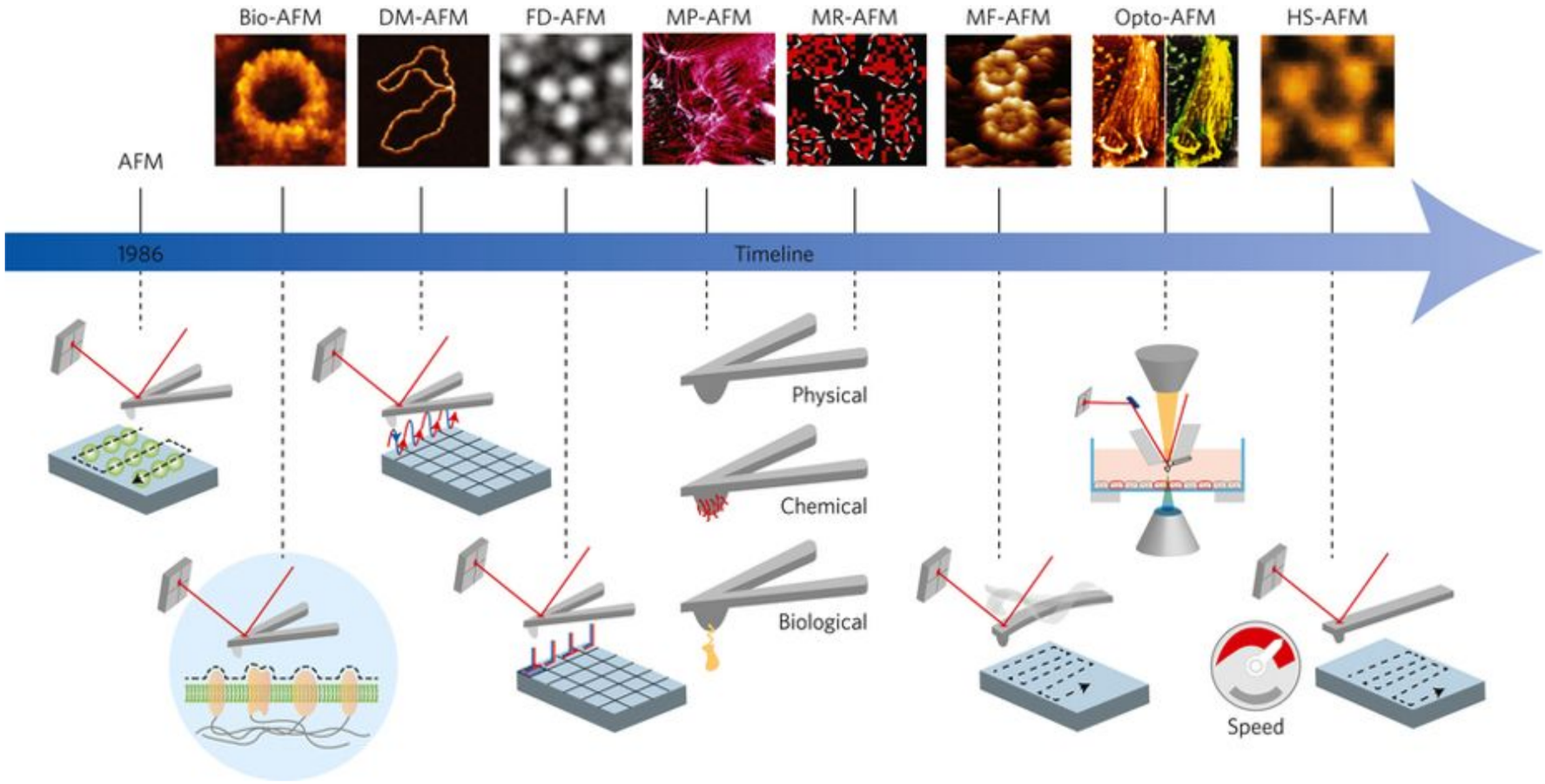

Key inventions developed over the years include: an optical detection system and fluid cell enabling contact mode AFM to operate in aqueous solution (Bio-AFM); dynamic mode AFM (DM-AFM), which oscillates the AFM tip to reduce friction while contouring the biological sample; force–distance curve-based AFM (FD-AFM), which contours the surface of a biological system while recording pixel-by-pixel a full force–distance curve; multiparametric AFM (MP-AFM), which contours the sample while mapping multiple physical or chemical properties; molecular recognition AFM (MR-AFM), which images and maps specific interactions of biological samples; multifrequency AFM (MF-AFM), which contours the sample while oscillating the cantilever tip at multiple frequencies, thus mapping various physical parameters; correlating advanced optical imaging and AFM (Opto-AFM) for the imaging of complex biological systems; high-speed AFM (HS-AFM), which speeds up the image acquisition time by a factor of ~1,000, providing access to dynamic processes in biology. Most modes cross-fertilized each other, ultimately leading to combinatorial AFM. Images adapted from: Bio-AFM, ref. 28, Macmillan Publishers Ltd; DM-AFM, ref. 45, American Chemical Society; FD-AFM, ref. 76, Wiley; MP-AFM, ref. 78, Elsevier; MR-AFM, ref. 9, Cell Press; MF-AFM, ref. 46, Macmillan Publishers Ltd; Opto-AFM, ref. 145, The Company of Biologists; HS-AFM, ref. 122, Macmillan Publishers Ltd.

https://doi.org/10.1038/nnano.2017.45

Measuring bilayer thickness by AFM

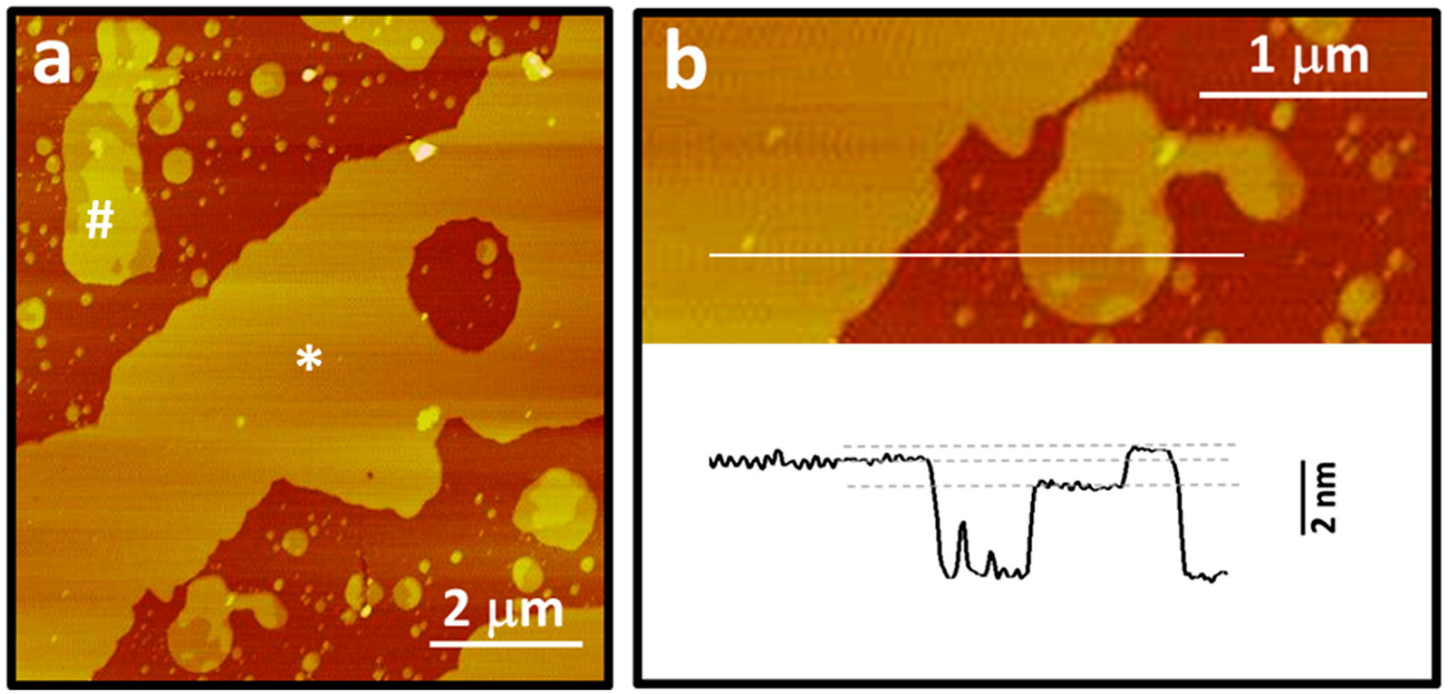

Fig. 2. AFM images of a DOPC/bSM/chol 1:1:1 supported lipid bilayer at 25 °C. a) The image shows homogeneous lipid bilayer patches (*) and smaller lipid bilayers in a phase coexistence state (#). b) Height difference between the homogeneous bilayer and the domains in a patch with phase coexistence. The height of the homogeneous bilayer is intermediate between the two domains in the small patch. The line section refers to the white line on the image. https://doi.org/10.1016/j.bbamem.2015.01.002

T_m dependency on headgroup, chain length, saturation

Avanti® Polar Lipids, Inc.

Phase Transition Temperatures for Glycerophospholipids

Phosphatidylcholine		Phosphatidylglycerol (Sodium Salt)	
Product	T_m (°C)	Product	T_m (°C)
12:0 PC (DLPC)	-2	12:0 PG (DLPG)	-3
13:0 PC	14	14:0 PG (DMPG)	23
14:0 PC (DMPC)	24	16:0 PG (DPPG)	41
15:0 PC	35	18:0 PG (DSPG)	55
16:0 PC (DPPC)	41	18:1 PG (DOPG)	-18
17:0 PC	50	16:0-18:1 PG (POPG)	-2
18:0 PC (DSPC)	55	**Phosphatidylserine (Sodium Salt)**	
19:0 PC	62	14:0 PS (DMPS)	35
20:0 PC	66	16:0 PS (DPPS)	54
21:0 PC	71	18:0 PS (DSPS)	68
22:0 PC	75	18:1 PS (DOPS)	-11
23:0 PC	79.5	16:0-18:1 PS (POPS)	14
24:0 PC	80.3	**Phosphatidic Acid (Sodium Salt)**	
16:1 PC	-36	12:0 PA (DLPA)	31
18:1c9 PC (DOPC)	-17	14:0 PA (DMPA)	52
18:1t9 PC	12	16:0 PA (DPPA)	65
18:1c6 PC	1	18:0 PA (DSPA)	75
22:1c13 PC	13	18:1 PA (DOPA)	-4
18:2 PC	-57	16:0-18:1 PA (POPA)	28
18:3 PC	-60	**Cardiolipin**	
		14:0 CL	47
		16:0 CL	62.2

(table continued)

Thermotropic Phase Transitions of Pure Lipids in Model Membranes and Their Modifications by Membrane Proteins, Dr. John R. Silvius, Lipid-Protein Interactions, John Wiley & Sons, Inc., New York, 1982. Reprinted with permission from John Wiley & Sons, Inc. Lipid Thermotropic Phase Transition Database (LIPIDAT) – NIST Standard Reference Database 34

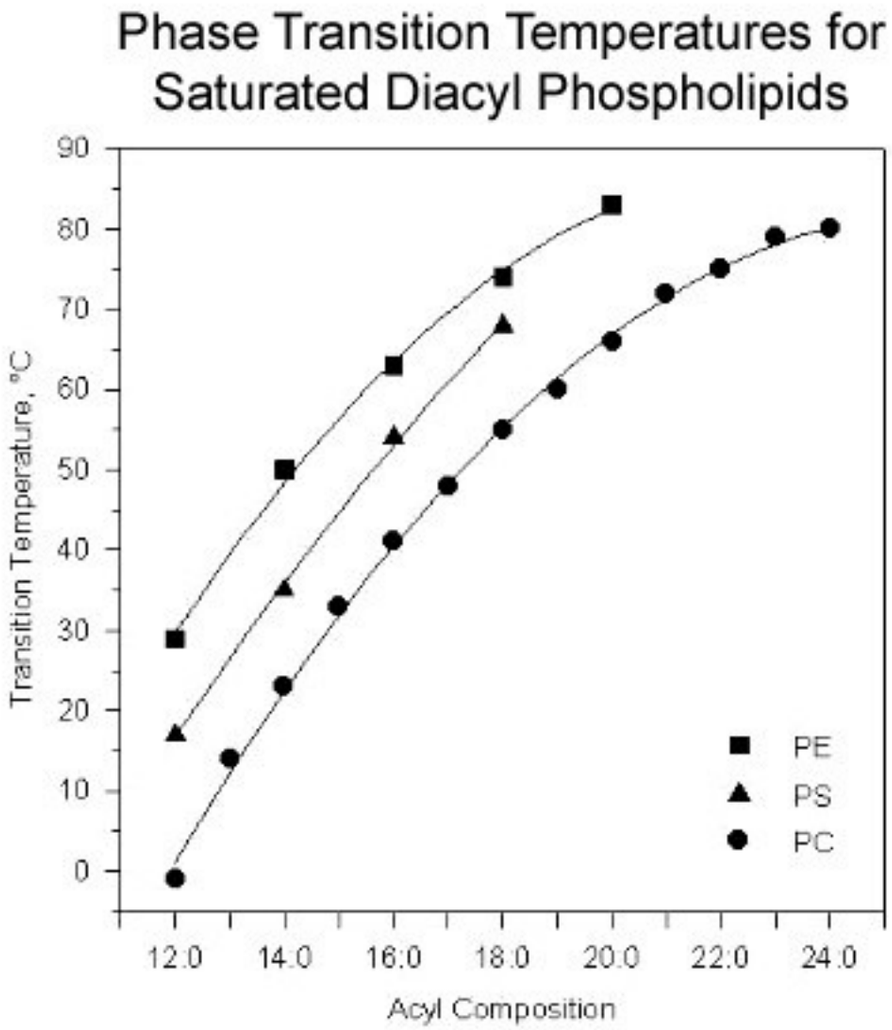

- **VDWs - tail length & saturation**
- **Head-group interactions with each other & water**
- **e.g. PE interacts with fewer waters which results in the ~30 degree increase in T_m**

T_m & chains • VDWs depend on tail length & saturation

DLPC
T_m = -2 °C

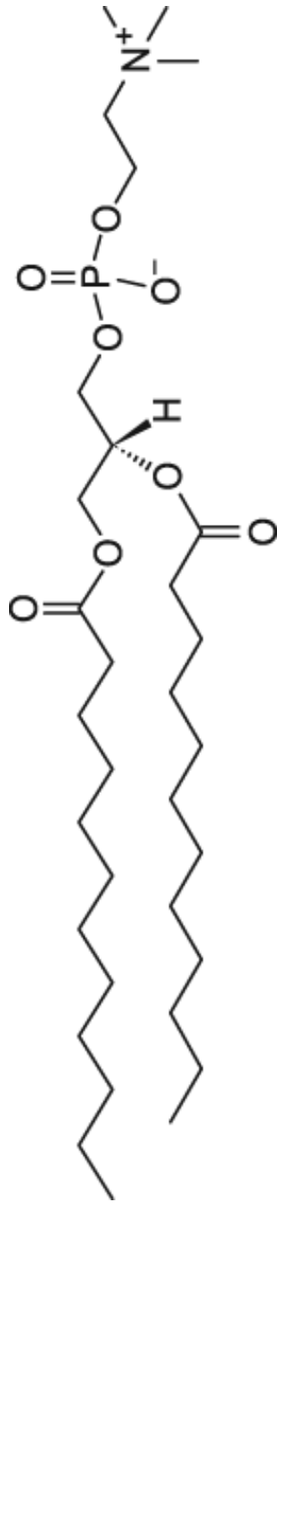

DMPC
T_m = 24 °C

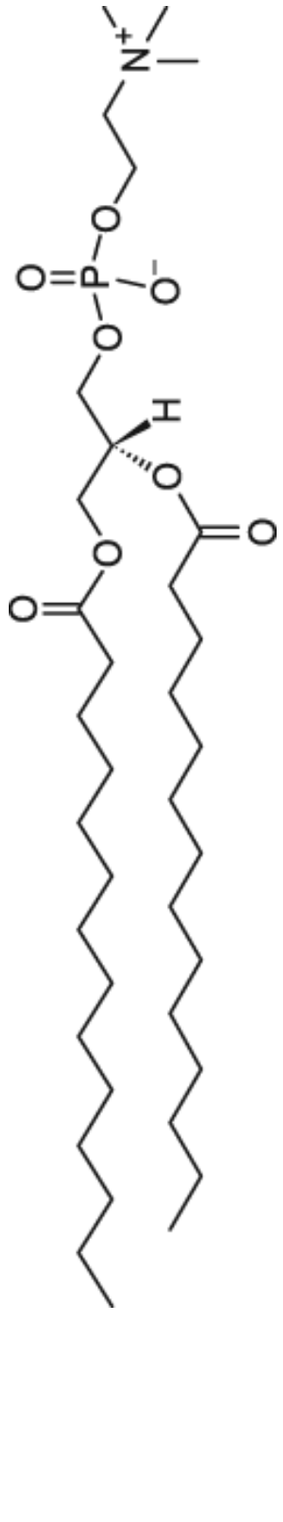

DPPC
T_m = 41 °C

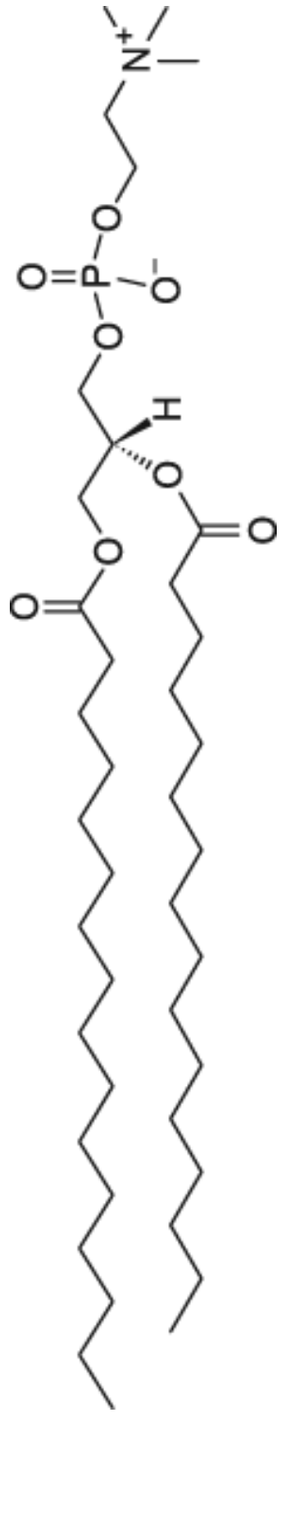

DSPC
T_m = 55 °C

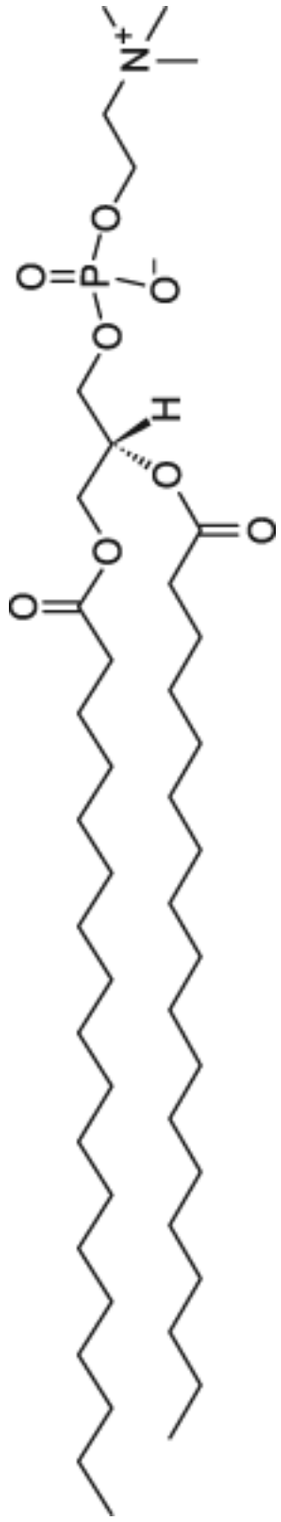

POPC
T_m = -2 °C

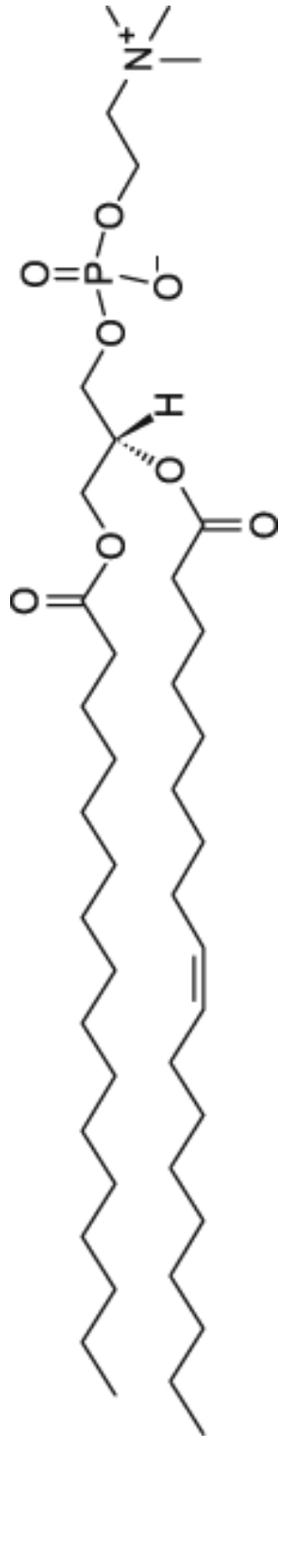

DOPC
T_m = -17 °C

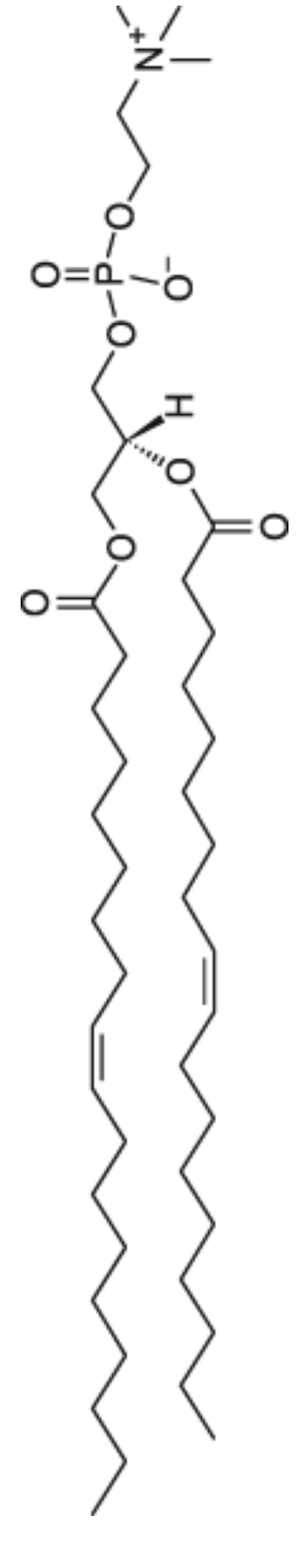

T_m & headgroup

- **Larger headgroups interact with more water and ions, decrease T_m**
- **Hydrogen bonding in PA & PE stabilize interlipid interactions, increase T_m**

POPA
T_m = 28 °C

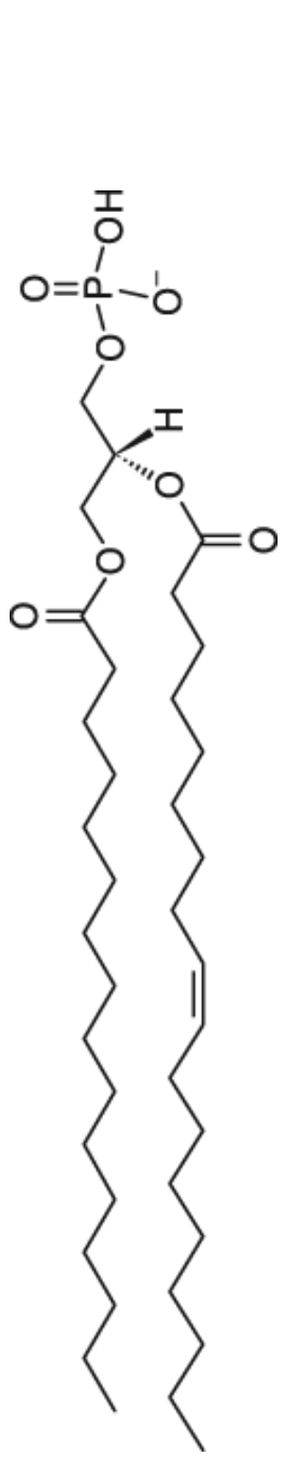

POPE
T_m = 25 °C

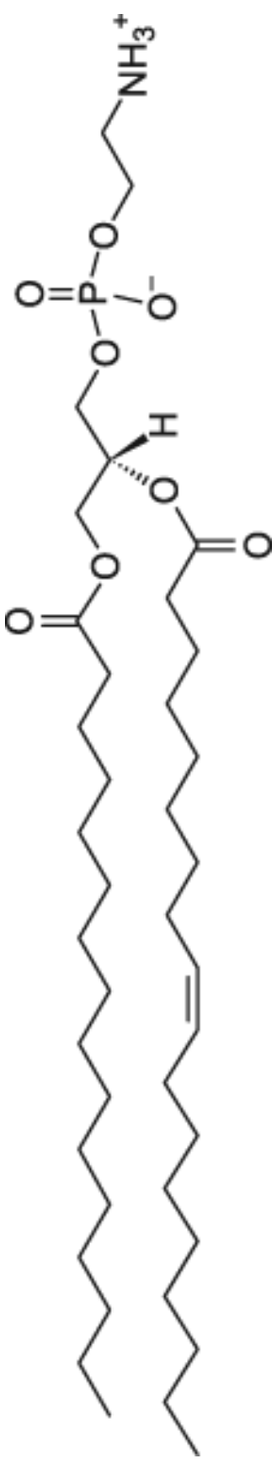

POPS
T_m = 14 °C

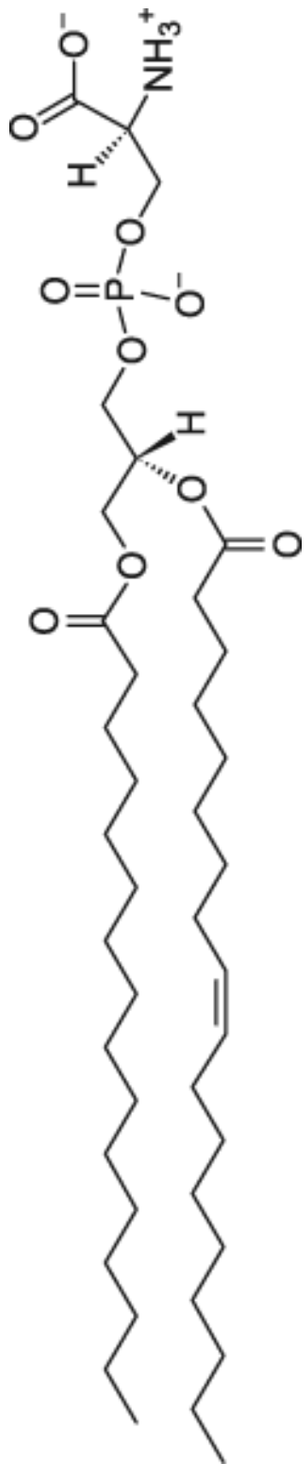

POPC
T_m = -2 °C

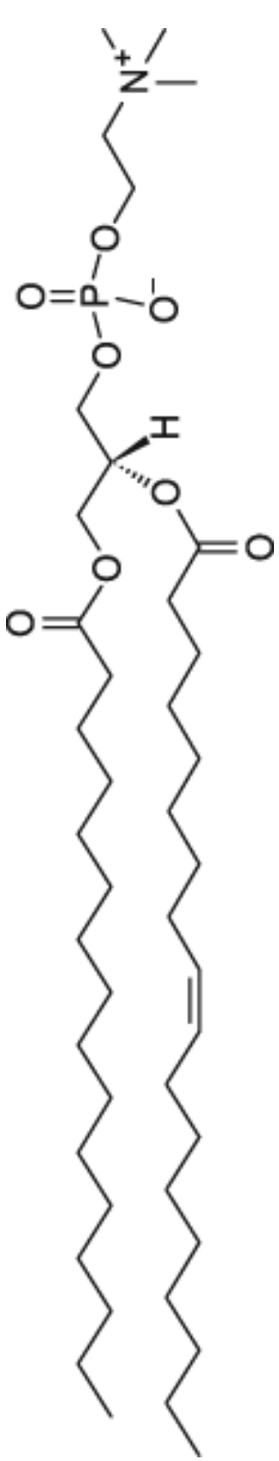

POPG
T_m = -2 °C

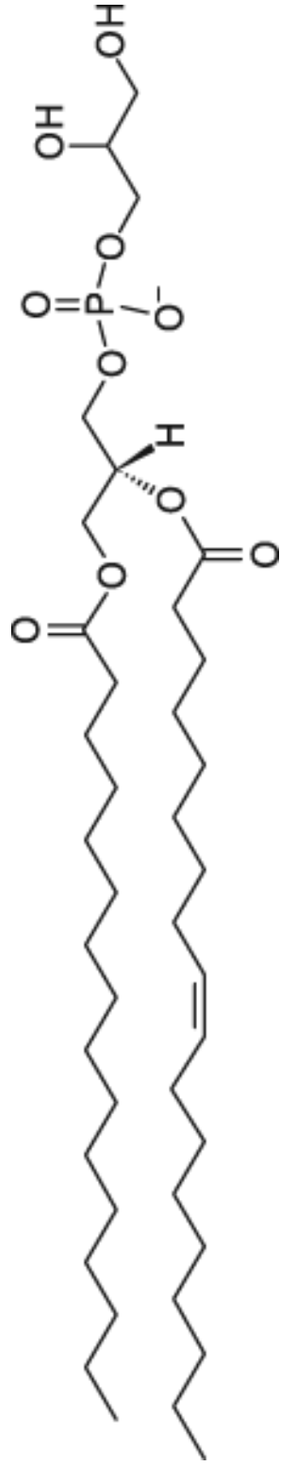

Lipid extraction & analysis

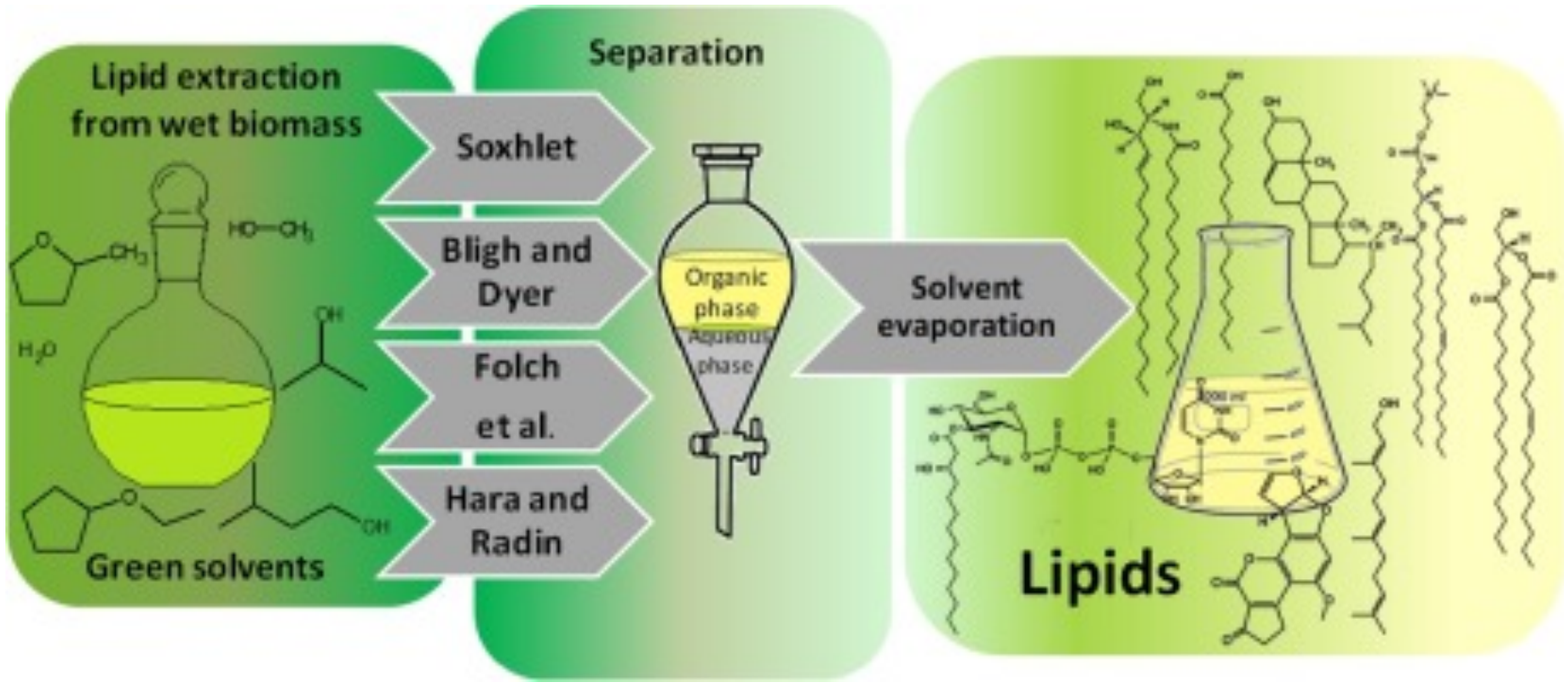

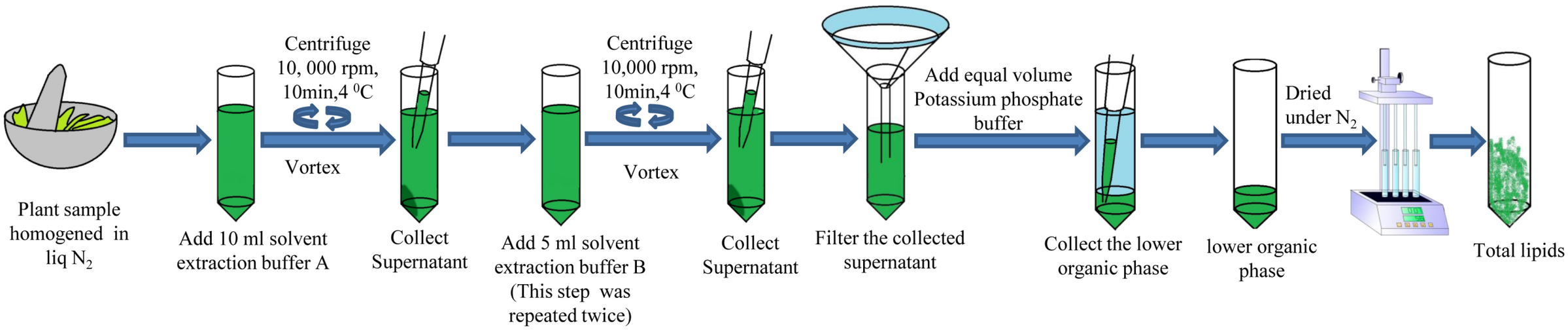

Bligh Dyer: chloroform/methanol/water 2:2:1.8 (v/v/v)

Folch: chloroform/methanol/water in a volumetric ratio of 8:4:3 (v/v/v)

https://avantilipids.com/product/100600

E. coli Polar Lipid Extract

This product is an extract of E. coli B (ATCC 11303) grown in Kornberg Minimal media at 37°C and taken at 3/4 log growth phase.
Total E. coli lipid extract is a chloroform:methanol extract of the respective tissue. This extract is partitioned against deionized water and the chloroform phase is concentrated.
Polar lipid extract is the total lipid extract precipitated with acetone and then extracted with diethyl ether.

E. coli Polar Extract Phospholipid Profile	
Component	wt/wt%
PE	67.0
PG	23.2
CA	9.8
Unknown	0.0
Total	100.0

E. coli Total Extract Phospholipid Profile	
Component	wt/wt%
PE	57.5
PG	15.1
CA	9.8
Unknown	17.6
Total	100.0

Biological phase transition temperatures

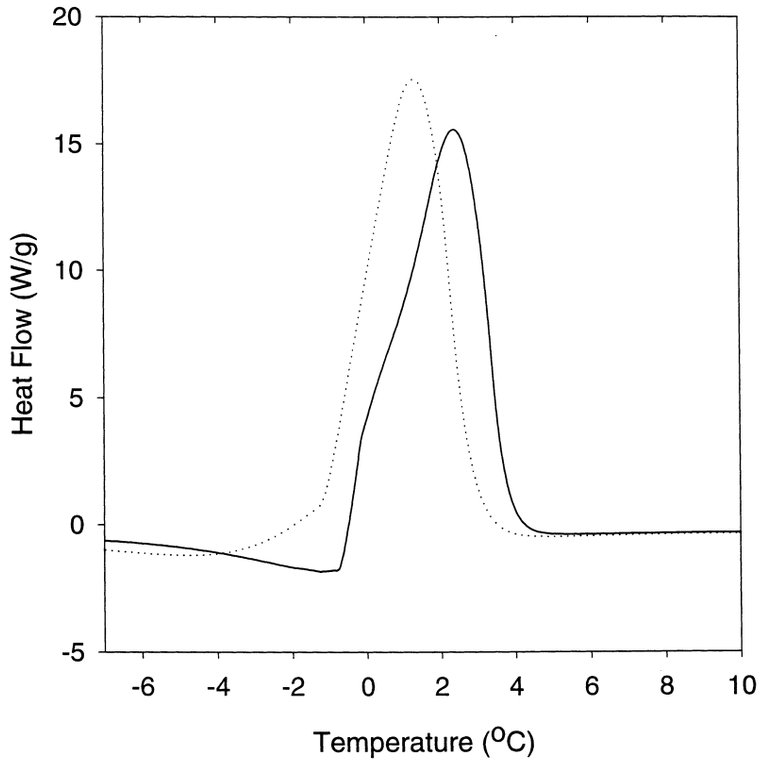

Fig. 2. Thermotropic phase transition of liposomes prepared with *E. coli* lipid. DSC was performed on liposomes prepared from *E. coli* lipid in phosphate buffer without (solid line) or supplemented with (dotted line) 0.30 M NaCl (see Section 2).

Physical properties of liposomes and proteoliposomes prepared from *Escherichia coli* polar lipids

Gisèle F. White [a], Kathleen I. Racher [b], André Lipski [c], F. Ross Hallett [a], Janet M. Wood [b,*]

[a] *Department of Physics, University of Guelph, Guelph, Ont., Canada N1G 2W1*
[b] *Department of Microbiology and Guelph-Waterloo Centre for Graduate Work in Chemistry and Biochemistry, University of Guelph, Guelph, Ont., Canada N1G 2W1*
[c] *Abteilung Mikrobiologie, Fachbereich Biologie/Chemie, Universität Osnabrück, D-49069 Osnabrück, Germany*

Received 30 August 1999; received in revised form 15 May 2000; accepted 1 June 2000

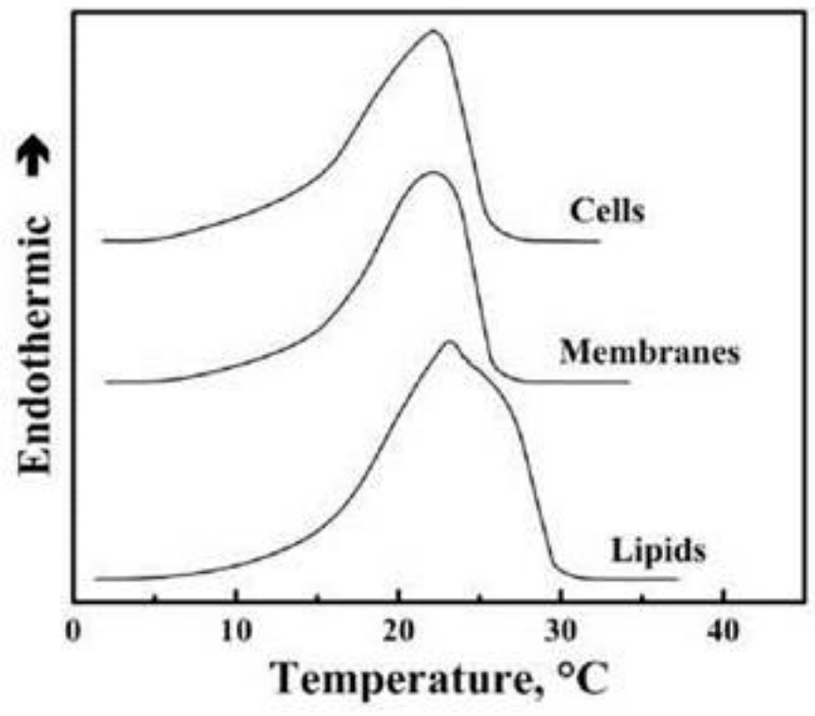

Figure 5. High-sensitivity DSC heating scans of Acholeplasma laidlawii B elaidic acid-homogeneous intact cells, isolated membranes and extracted total membrane lipids dispersed as multilamellar vesicles in water.

doi: 10.1002/9780470048672.wecb049

Phase transitions in mixed bilayers are shifted and broad

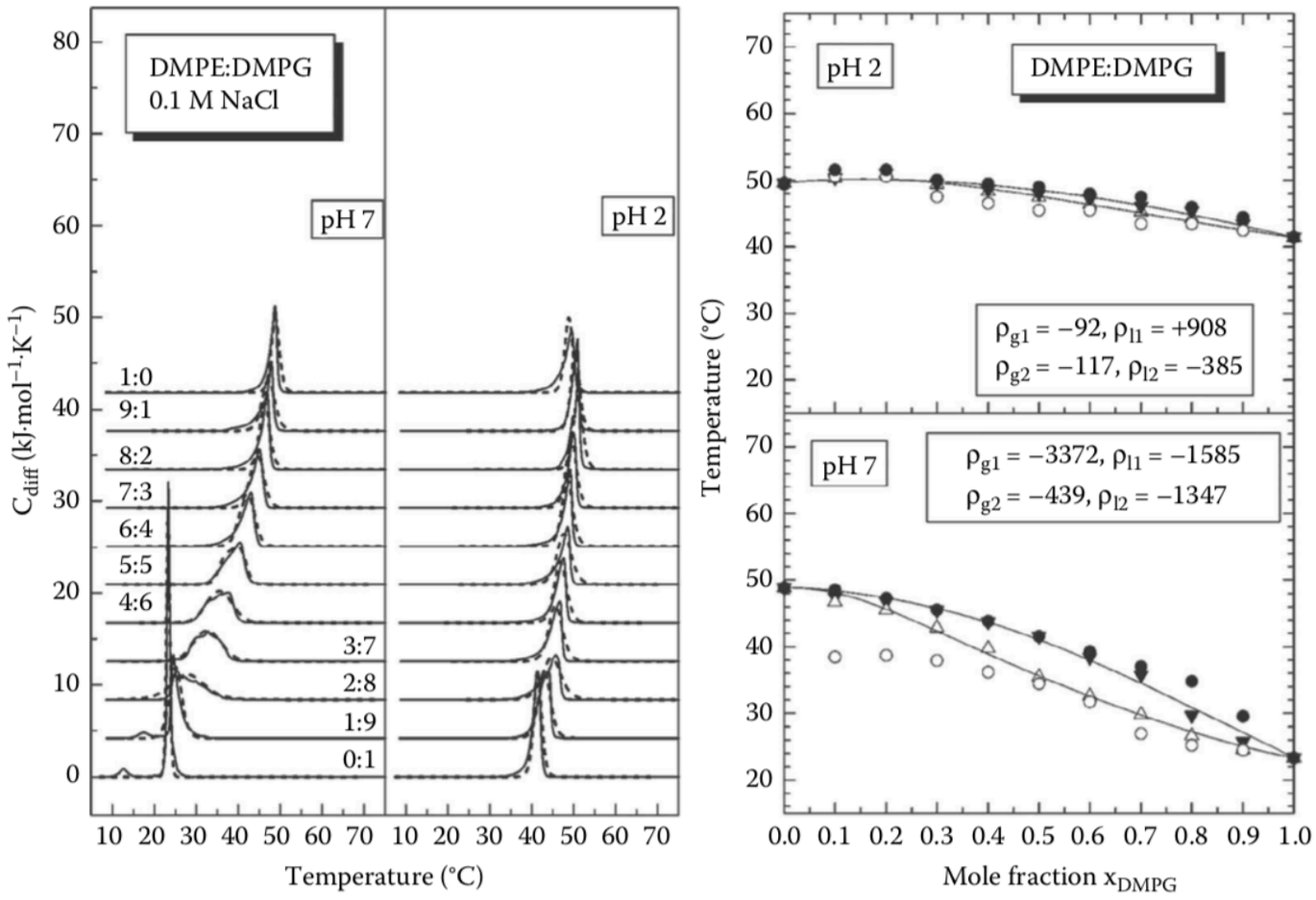

FIGURE 6.8 (a) DSC curves of mixtures of DMPE with DMPG in 0.1 M NaCl at two different pH values and various molar ratios. Solid line: experimental C_p curves; dotted line: simulated C_p curves. At pH = 2, the PG headgroup is almost completely protonated. (b) Pseudo-binary phase diagrams for the DMPE:DMPG system at pH 2 and 7. Triangles are T(–) and T(+) values obtained from the simulation of the C_p curve; circles are Texp(–) and Texp(+) values obtained by the usual empirical procedure. The solid lines are the coexistence lines obtained by a nonlinear least square fit of the T(–) and T(+) values using the four-parameter nonideal, nonsymmetric mixing model, yielding the nonideality parameters as indicated. (Adapted from Garidel, P., and Blume A., *Eur. Biophys. J.* 28, 629–638, 2000.)

2D Ising models can predict phase transition temperatures

LANGMUIR

Cite This: *Langmuir* 2019, 35, 21−40

Invited Feature Article

pubs.acs.org/Langmuir

How to Determine Lipid Interactions in Membranes from Experiment Through the Ising Model

Paulo F. Almeida*

Department of Chemistry and Biochemistry, University of North Carolina Wilmington, Wilmington, North Carolina 28403, United States

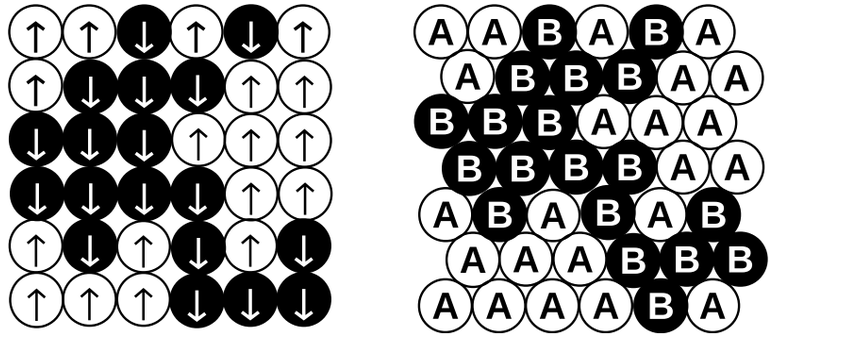

Figure 3. (left) Up and down spins in a square lattice. (right) Two lipid species A and B in a triangular lattice.

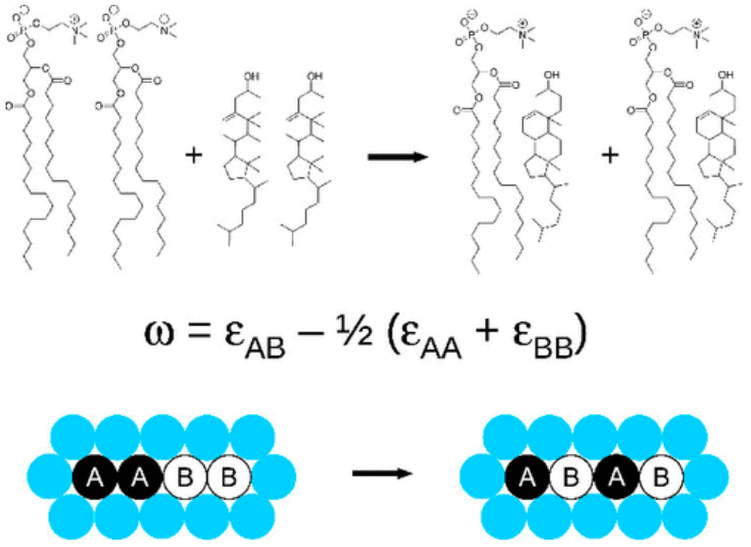

Table 1. Physical Properties of DPPC Vesicles

vesicle	diameter (μm)	T_m (°C)	ΔH (kcal/mol)	ΔC_p (kcal/K/mol)	ω (cal/mol)	refs
MLV	1−10	41.4	8.7	∼10−100	∼350	17, 68−70
GUV	∼10	41.7	8.7	5.0	310	71
LUV	0.1	40.8	8.7	3.5	300	17, 22, 72, 73
SUV	0.02	37.2	8.7	2.0	280	12, 16, 17

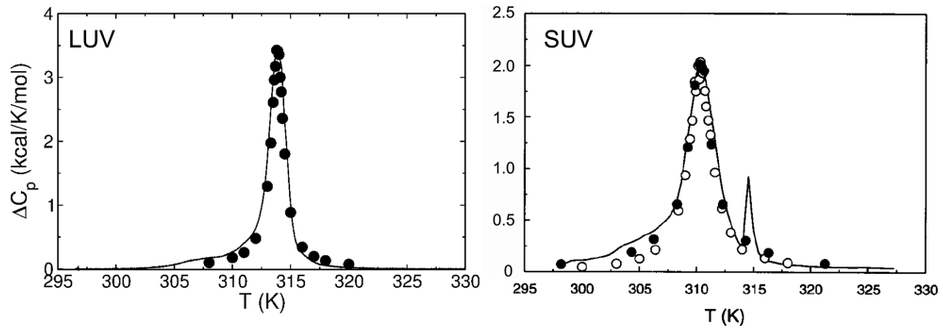

Figure 6. Heat capacity of DPPC LUVs and SUVs measured experimentally by DSC (lines) and calculated by Monte Carlo simulations of the Ising model (points). LUV (left) The experimental data are from Ivanova and Heimburg,[17] courtesy of Dr. Heimburg, renormalized slightly to our average ΔC_p^{max} and T_m values. The simulations are from Svetlovics et al.[18] SUV (right) Reprinted with permission from Jerala et al.[12] Copyright 1996 The Biophysical Society. The solid symbols are from simulations where each site represents a lipid molecule. The open symbols are from simulations where each site represents an acyl chain, connected to one of its neighbors to form a whole lipid. The sharp peak at high temperature is from residual MLVs in the sample, which are extremely difficult to eliminate completely because of fusion of the highly strained SUVs.[69]

Cholesterol and membrane fluidity

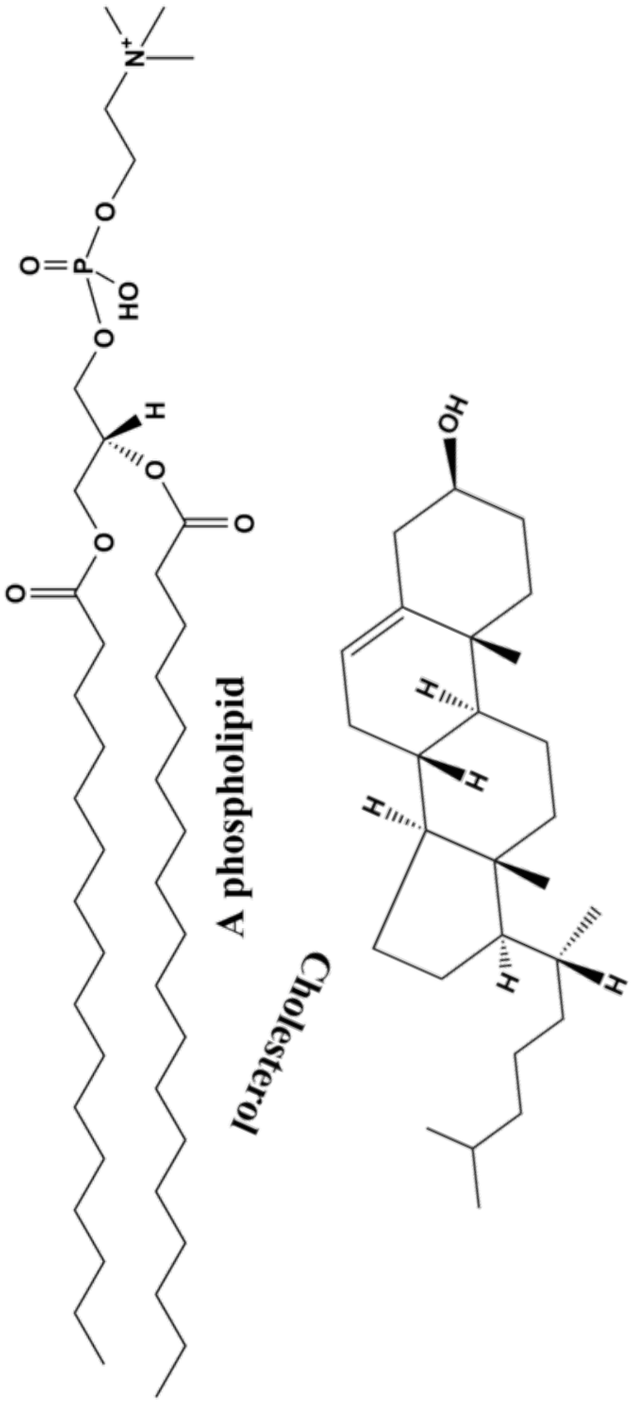

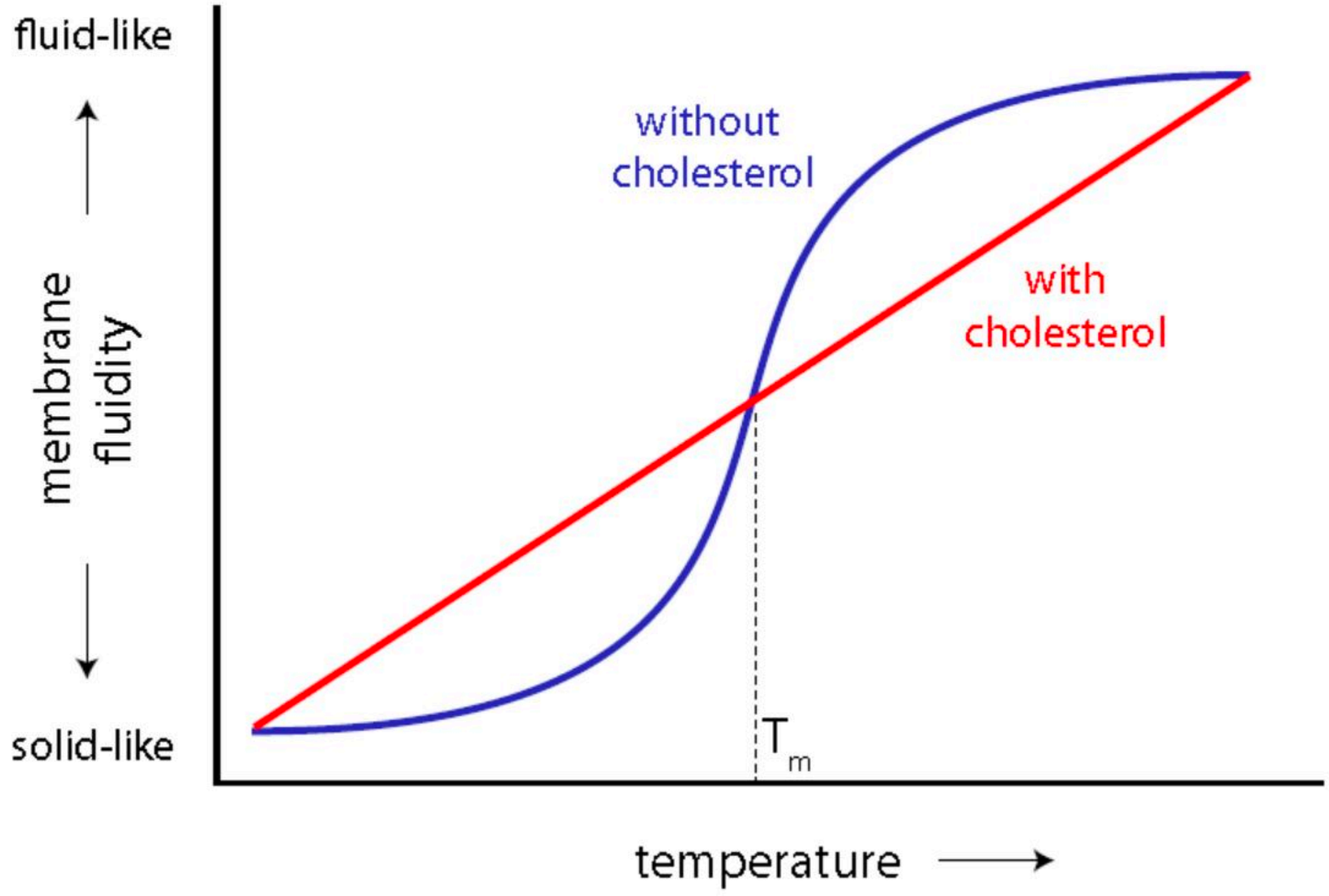

https://www.labxchange.org/library/pathway/lx-pathway:27cf60e0-851b-4261-ba07-42405b3c8e8e/items/lx-pb:27cf60e0-851b-4261-ba07-42405b3c8e8e:html:926cb1c7

Lipid diffusion in different membrane phases

- Lipids in gel membranes are not frozen in time, but move slower - think bacon grease
- Different phases can coexist within the same bilayer, depending on the lipids involved
- Addition of cholesterol promotes the liquid ordered phase

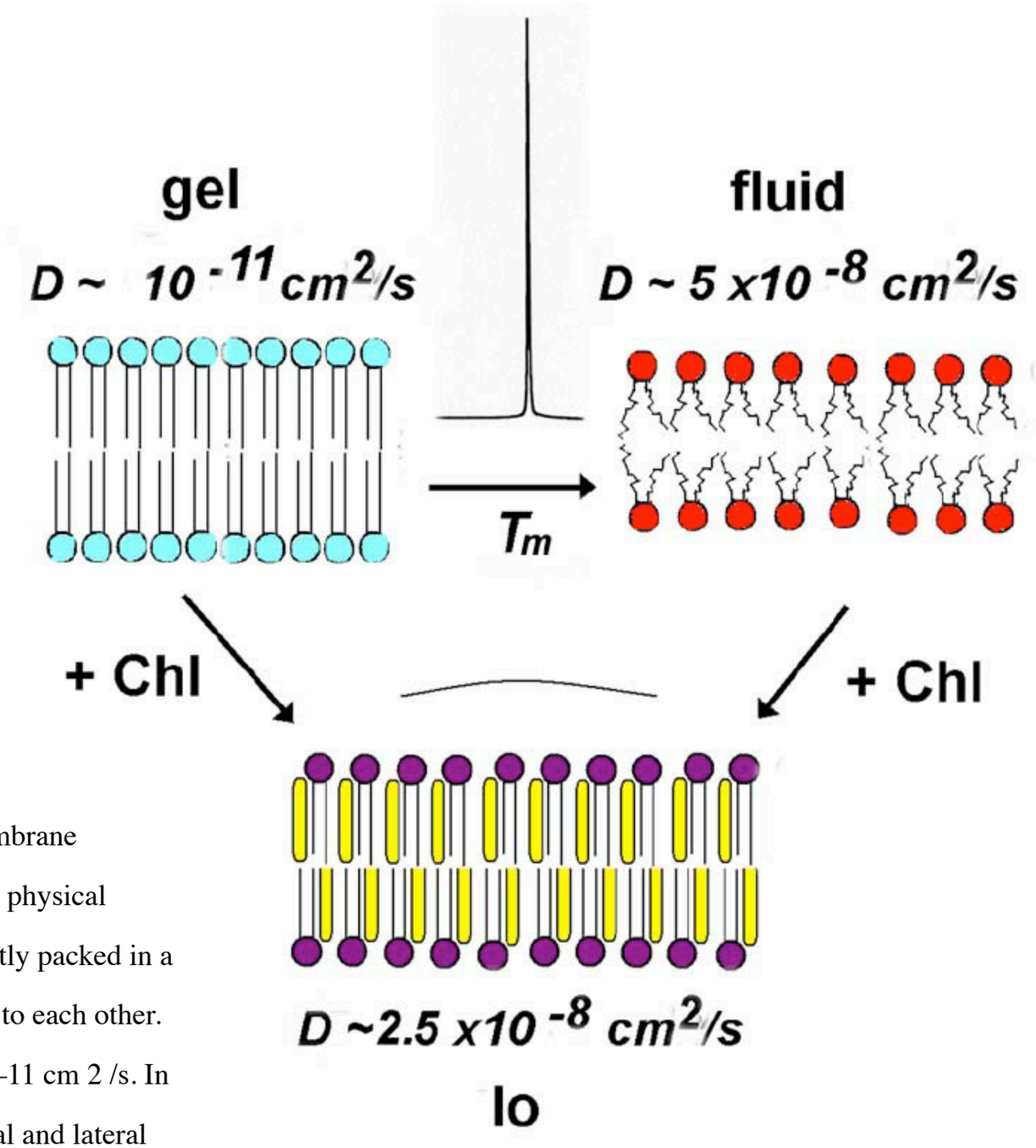

Phase behavior of phospholipids. In the presence of aqueous buffer, a majority of membrane phospholipids form spontaneously solvated lipid bilayers that can exist in two distinct physical states, gel and fluid, according to the temperature. In the gel phase, molecules are tightly packed in a quasi-hexagonal array with their extended and ordered fatty acid chains lying parallel to each other. Intra- and intermolecular motions are slow, with lateral diffusion coefficient D < 10 ^–11 cm 2 /s. In the fluid phase, acyl chains are highly mobile and the molecules undergo fast rotational and lateral (D) diffusion. This is accompanied by a thinning of the bilayer. https://www.researchgate.net/figure/Phase-behavior-of-phospholipids-In-the-presence-of-aqueous-buffer-a-majority-of_fig1_10709024

Coexistence of Lo & Ld

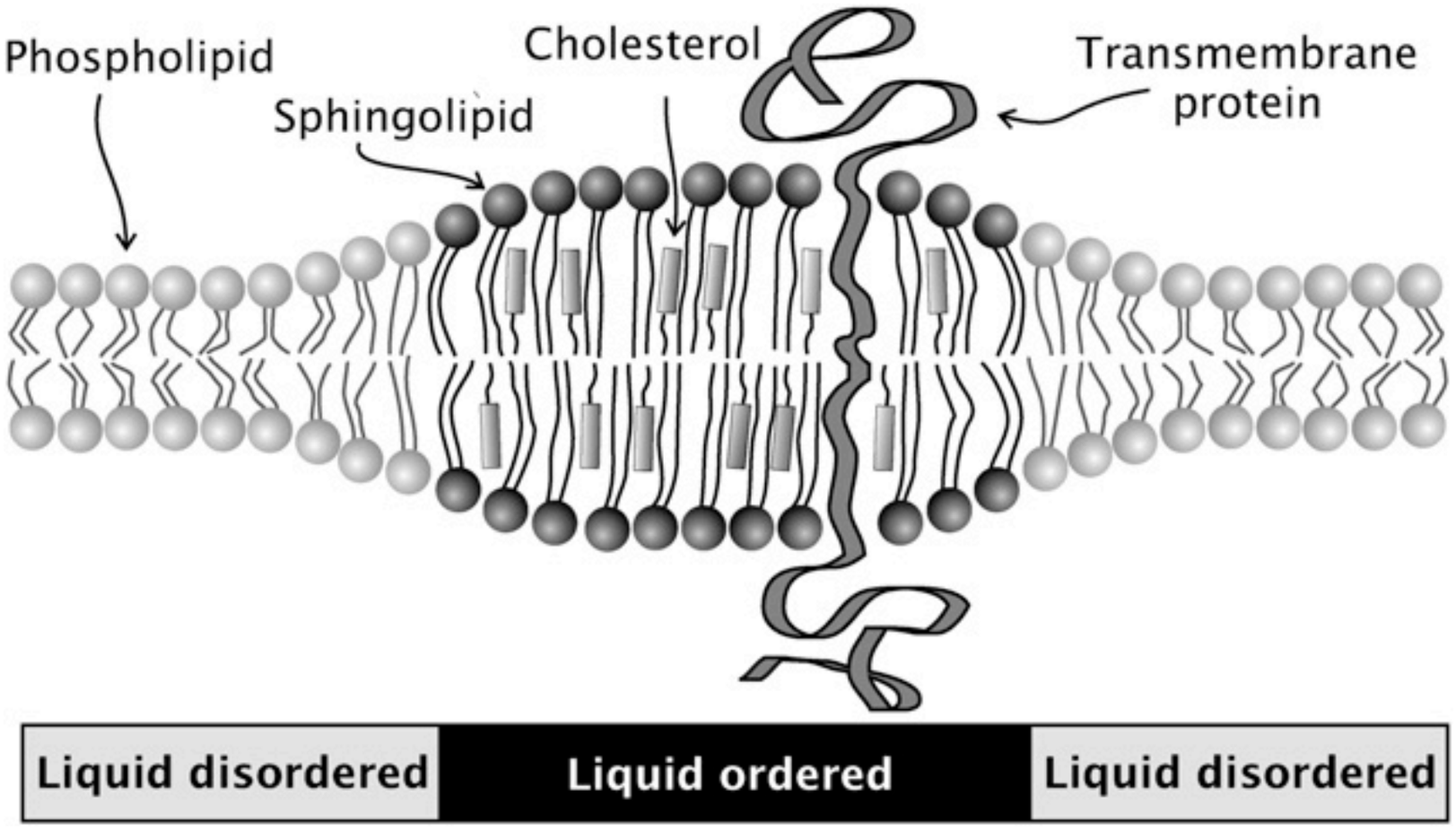

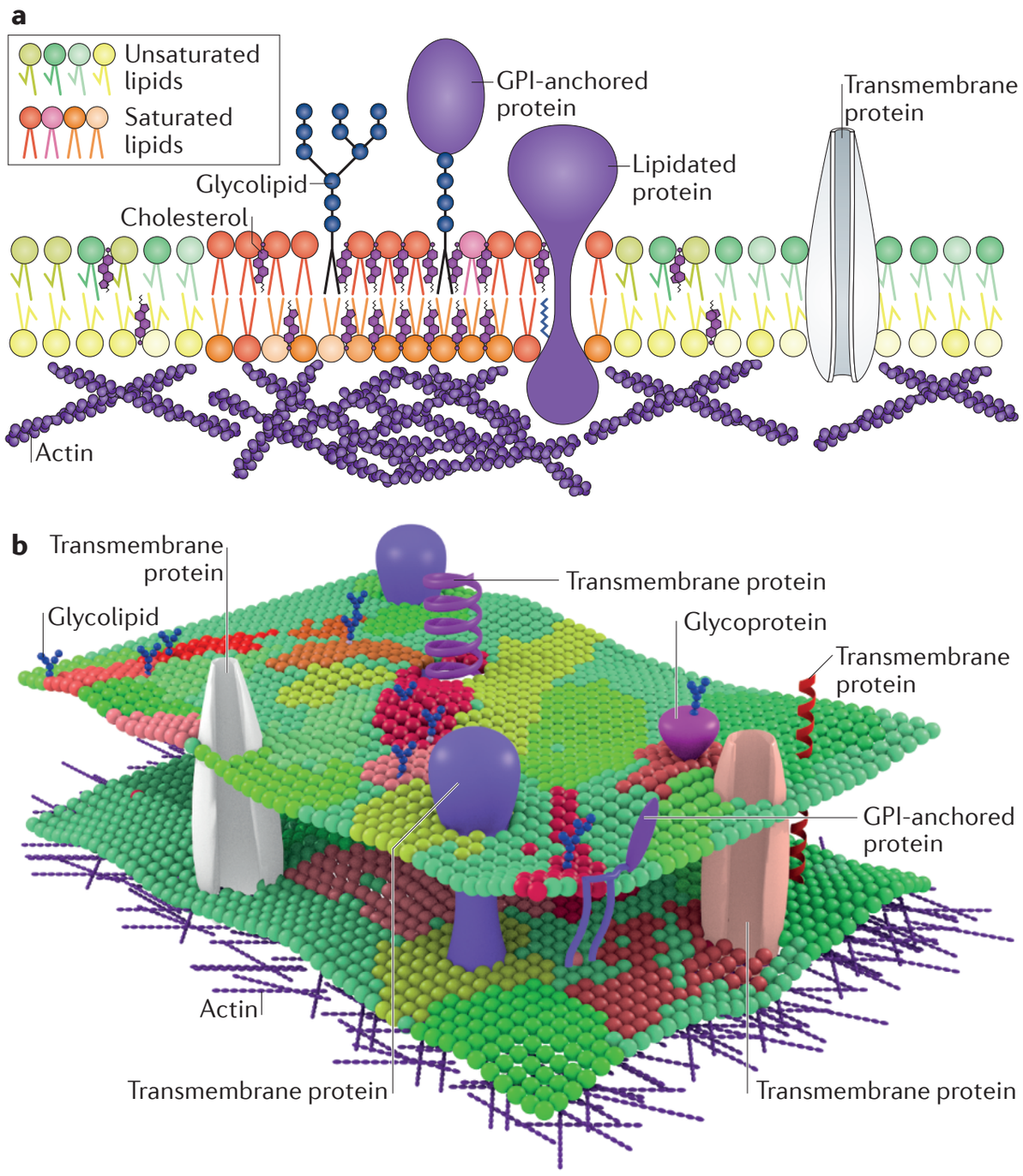

Figure 1 | **General overview of lateral heterogeneity in the plasma membrane.** **a** | Lipid raft domains are usually defined as small, highly dynamic and transient plasma membrane entities that are enriched in saturated phospholipids, sphingolipids, glycolipids, cholesterol, lipidated proteins and glycosylphosphatidylinositol (GPI)-anchored proteins. Enrichment of these hydrophobic components endows these lipid domains with distinct physical properties; these include increased lipid packing and order, and decreased fluidity. In addition to membrane components, cortical actin plays an active part in domain maintenance and remodelling. Furthermore, membrane lipids are asymmetrically distributed in the inner and outer leaflets, which may further affect membrane organization. **b** | It is likely that membrane organization is not binary (that is, highly distinct raft and non-raft regions), but instead membranes consist of various raft-like and non-raft domains with distinct compositions and properties.

Measuring lipid dynamics and order by ^2H NMR

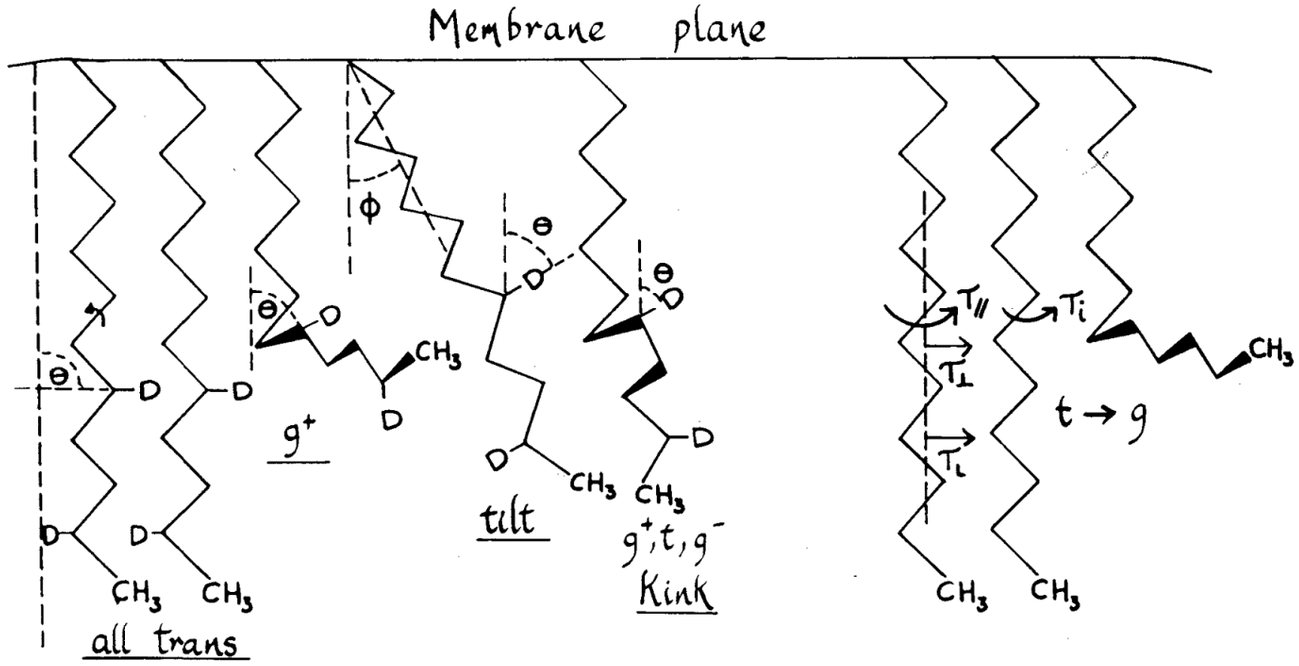

Figure 1. Schematic of the parameters used to characterize the degree of order and mobility of the fatty acyl chains of membrane lipids. The angle θ describes the instantaneous angle made by a C-D (C-^{2}H) bond with respect to the axis about which the lipids are ordered, whereas ϕ describes a possible tilting of the long molecular axes of the chains with respect to the normal. The correlation times τ are for the various possible motions of the chains: $\tau_{\parallel}$, motion about the long molecular axis; $\tau_{\perp}$, motion normal to the long axis; τ_L, lateral motion of the entire molecule parallel to the membrane surface; τ_i, rotation about the ith C-C single bond such as is involved in *trans-gauche* conformation interconversion. Note the representation of a kink, a *gauche*$^+$-*trans*-*gauche*$^-$ conformational triad.

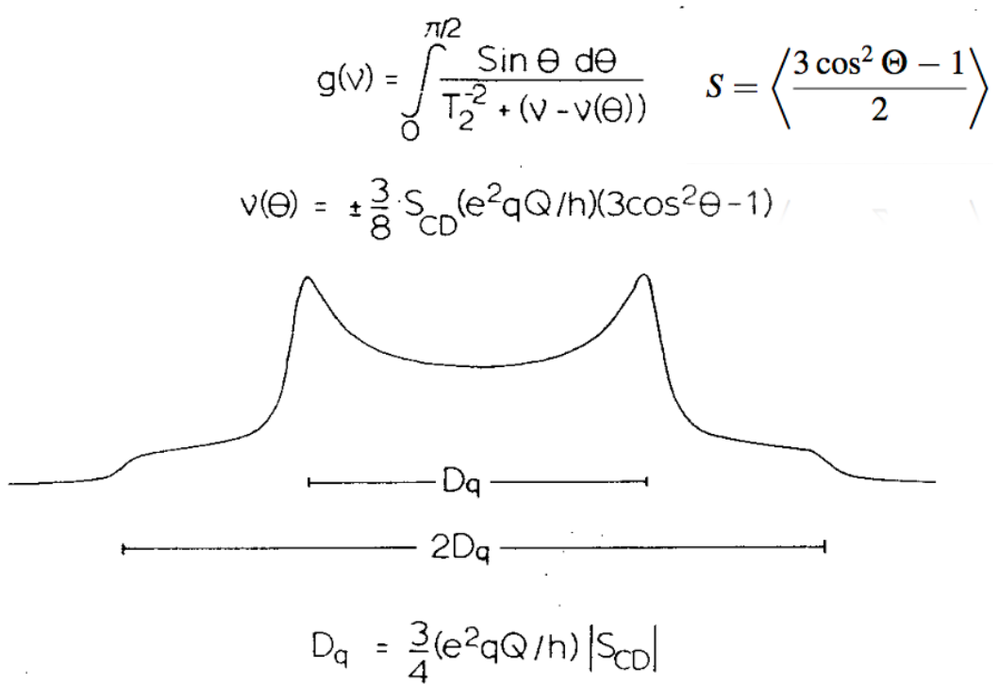

Figure 2. A theoretical ^{2}H NMR powder pattern for a C-^{2}H bond in a partially ordered system which, like a biological membrane, rotates slowly on the time scale of deuterium quadrupole splittings. The spectrum $g(\nu)$ is an envelope of the many spectra $\nu(\theta)$ for different orientations of the C-^{2}H bond with respect to the applied magnetic field of the spectrometer. The separation D_q gives a direct measure of the segmental order parameter, S_{CD}.

The states of the lipids in biological membranes as visualized by deuterium NMR, Smith, 1981, Bull. Man Reson. 3:120

- Protons in lipids can be replaced by deuterium atoms
- NMR provides information on the order and mobility of the molecule
- S_{CD} order parameter can be calculated from quadrupolar splitting
- R - relaxation parameters can inform on intramolecular dynamics

Quantification of phase separation by 2H NMR

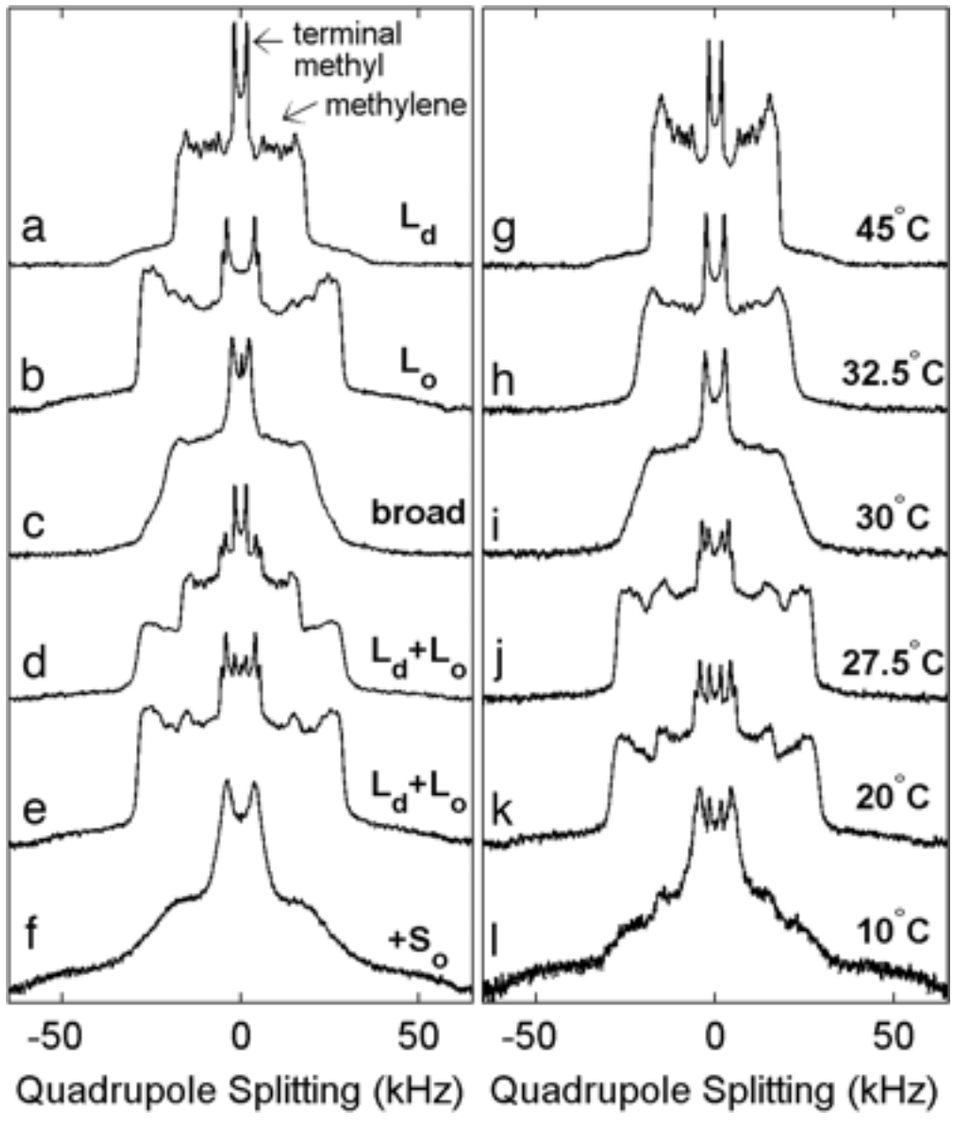

^{2}H NMR spectra of DPPC-d_{62} in membranes of DOPC/DPPC-d_{62}/Chol. (*a*–*f*) ^{2}H NMR spectra of DPPC-d_{62} in multilamellar vesicles of various DOPC/DPPC-d_{62}/Chol compositions acquired at 20°C with phase assignments as described in the text. Membrane compositions are in the form DOPC:DPPC-d_{62} plus % Chol: *a*, 4:1 plus 15%; *b*, 4:1 plus 40%; *c*, 2:1 plus 25%; *d*, 1:1 plus 15%; *e*, 1:2 plus 25%; *f*, 1:4 plus 10%. (*g*–*l*) Spectra for membranes of 1:2 DOPC/DPPC-d_{62} plus 20% Chol at the temperatures indicated.

https://doi.org/10.1073/pnas.0703513104

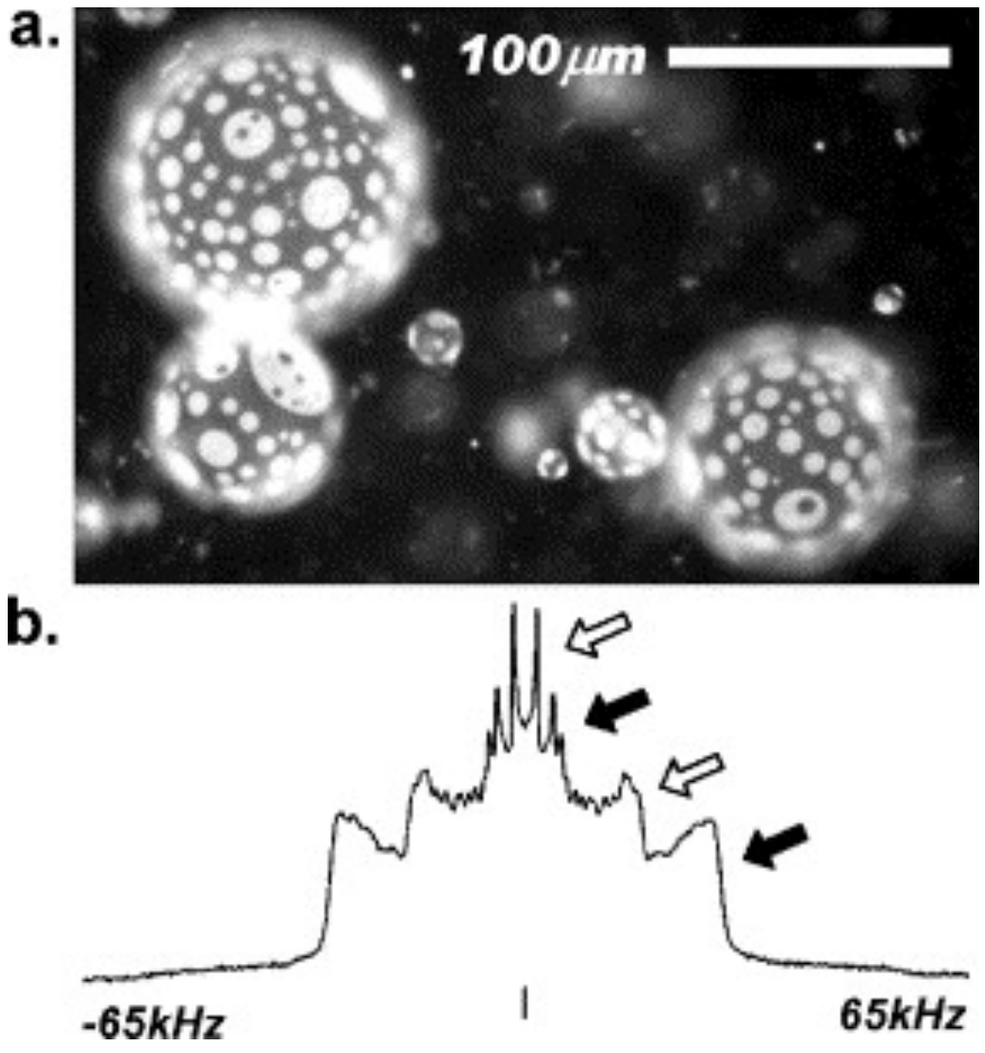

Fig. 1. (a) Immiscible liquid phases are directly visualized on the surface of giant unilamellar vesicles by fluorescence microscopy. (b) Distinct superposition of ^{2}H NMR spectra demonstrates that liquid-crystalline (L_α) and liquid-ordered (L_o) phases coexist in vesicle membranes. Distinguishing features of L_α (L_o) spectra are denoted by white (black) arrows as described in [54]. Membrane compositions are (a) 1:1 DPhyPC/DPPC + 50% cholesterol at 26 °C and (b) 1:1 DOPC/DPPCd62 + 20% cholesterol at 20 °C.

Veatch & Keller, BBA - Molecular Cell Research, 2005

https://doi.org/10.1016/j.bbamcr.2005.06.010

Lipid phase diagrams of mixed systems

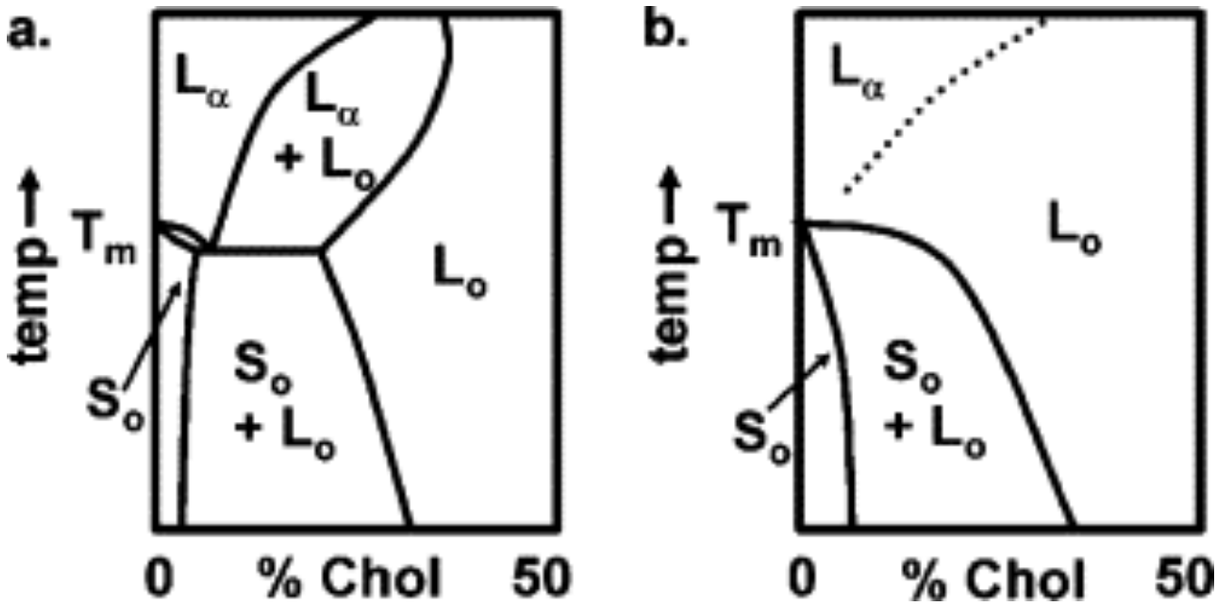

Fig. 6. Phase diagrams proposed in the literature for bilayer membranes containing binary mixtures of phospholipids and cholesterol. Diagrams in (a and b) differ in their description of phases above T_m. In (a), regions of L_α and L_o phases are separated by a coexistence region. Diagram (b) depicts a gradual transition between L_o and L_α phases (denoted by the dotted line). There is support for both types of diagrams in the literature (see text).

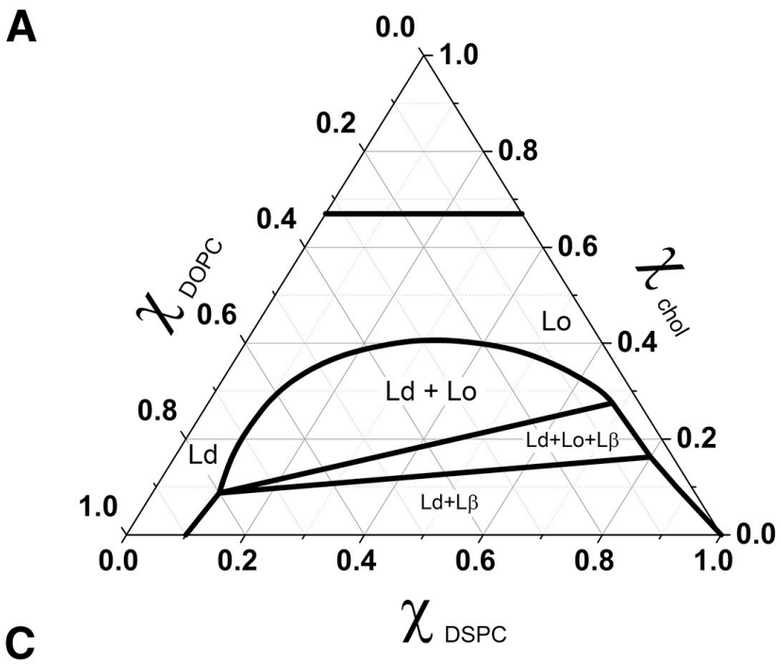

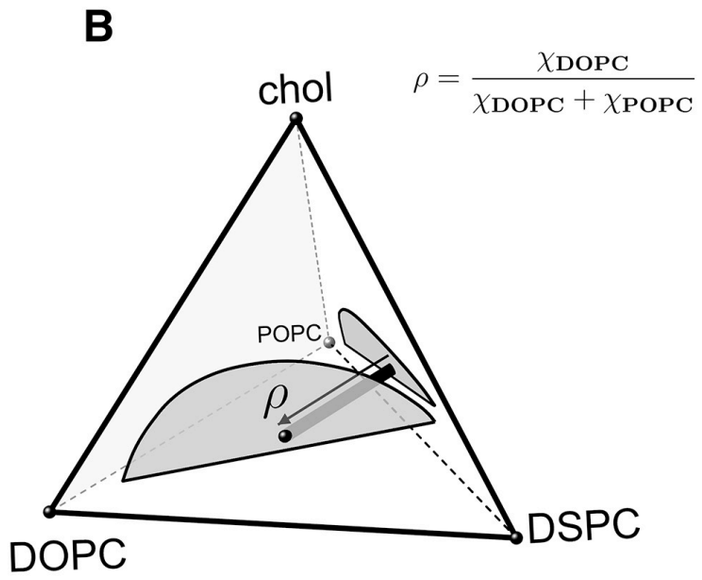

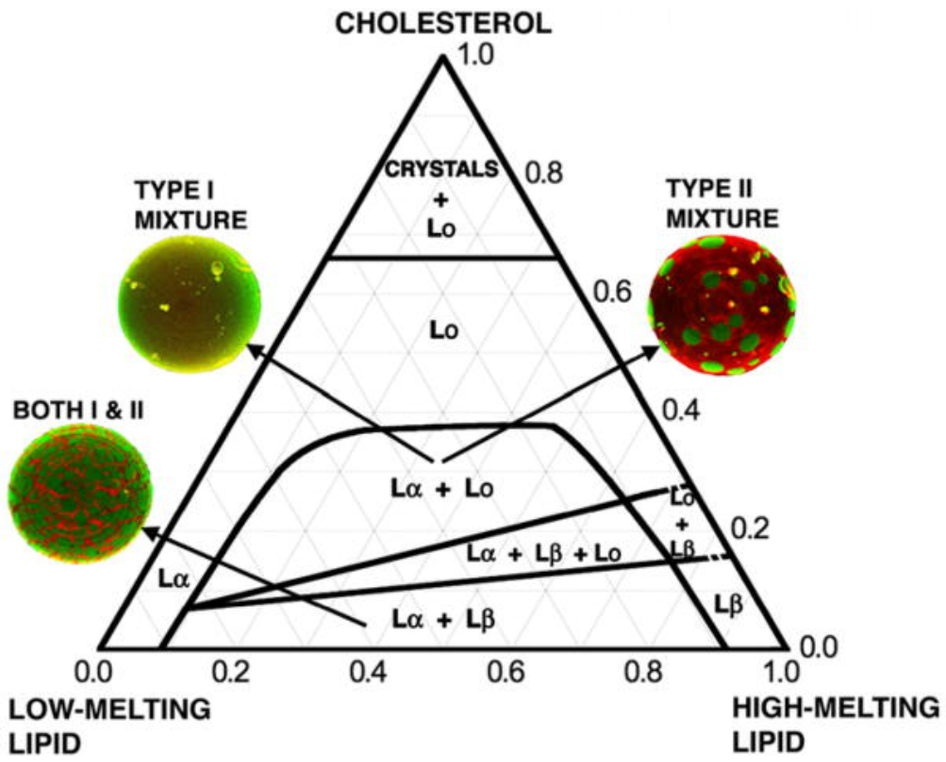

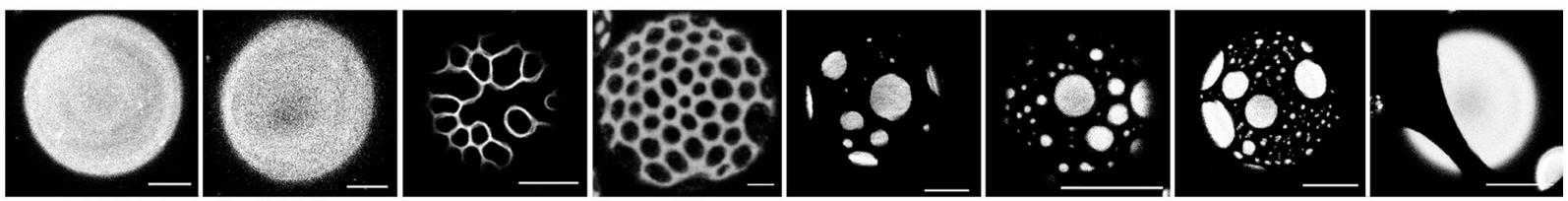

https://doi.org/10.1016/j.bpj.2017.02.033

Lipid phases in biological membranes via microscopy

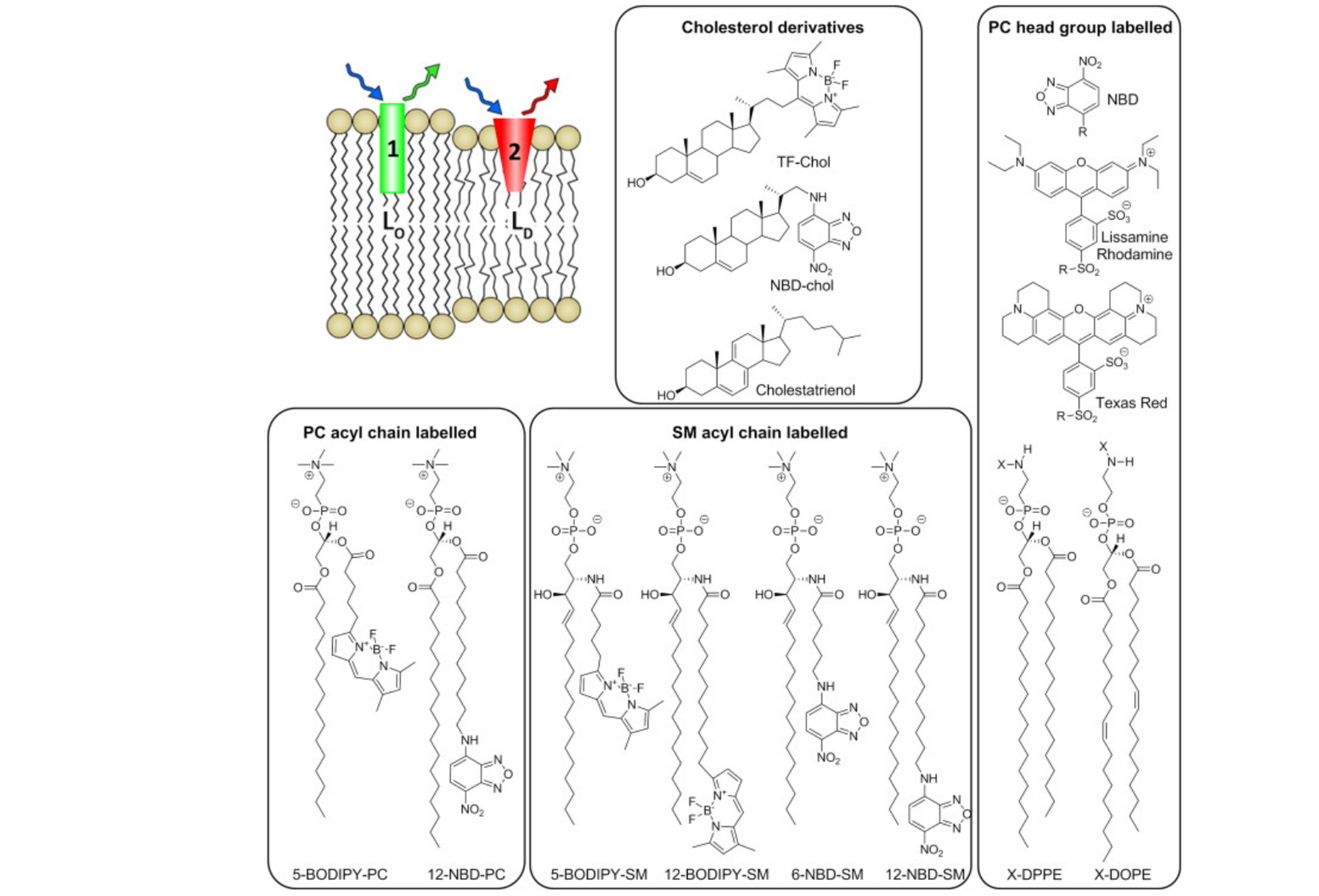

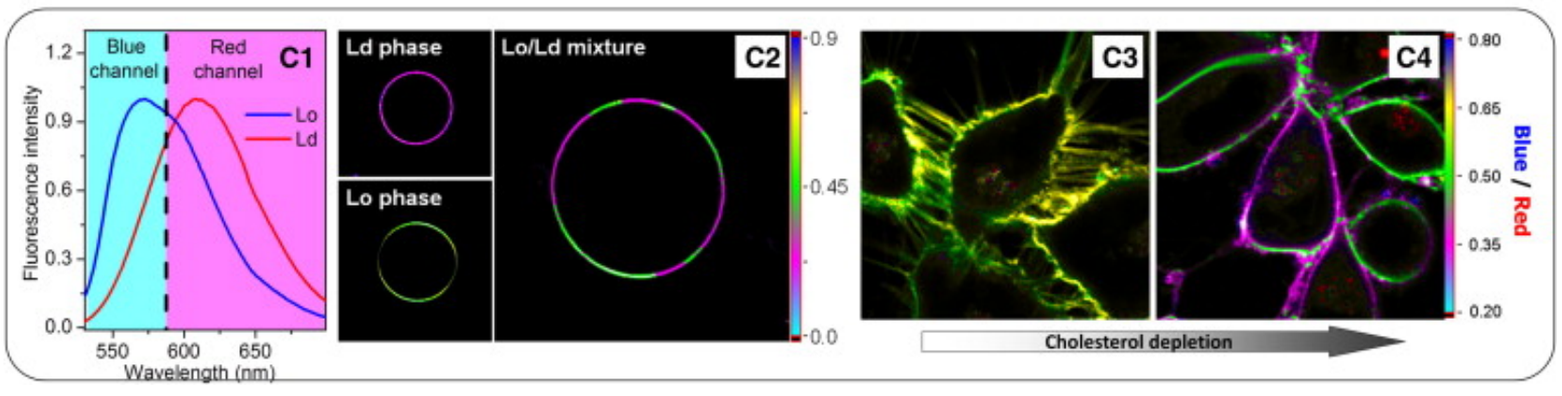

https://doi.org/10.1016/j.chembiol.2013.11.009

Measuring lipid diffusion - Fluorescent Recovery After Photobleaching (FRAP)

MOBILITY MEASUREMENT BY
ANALYSIS OF FLUORESCENCE
PHOTOBLEACHING RECOVERY KINETICS

D. AXELROD, D. E. KOPPEL, J. SCHLESSINGER, E. ELSON, *and* W. W. WEBB

From the School of Applied and Engineering Physics, and Department of Chemistry, Cornell University, Ithaca, New York 14853

BIOPHYSICAL JOURNAL VOLUME 16 1976

doi: [10.1016/S0006-3495(76)85755-4]

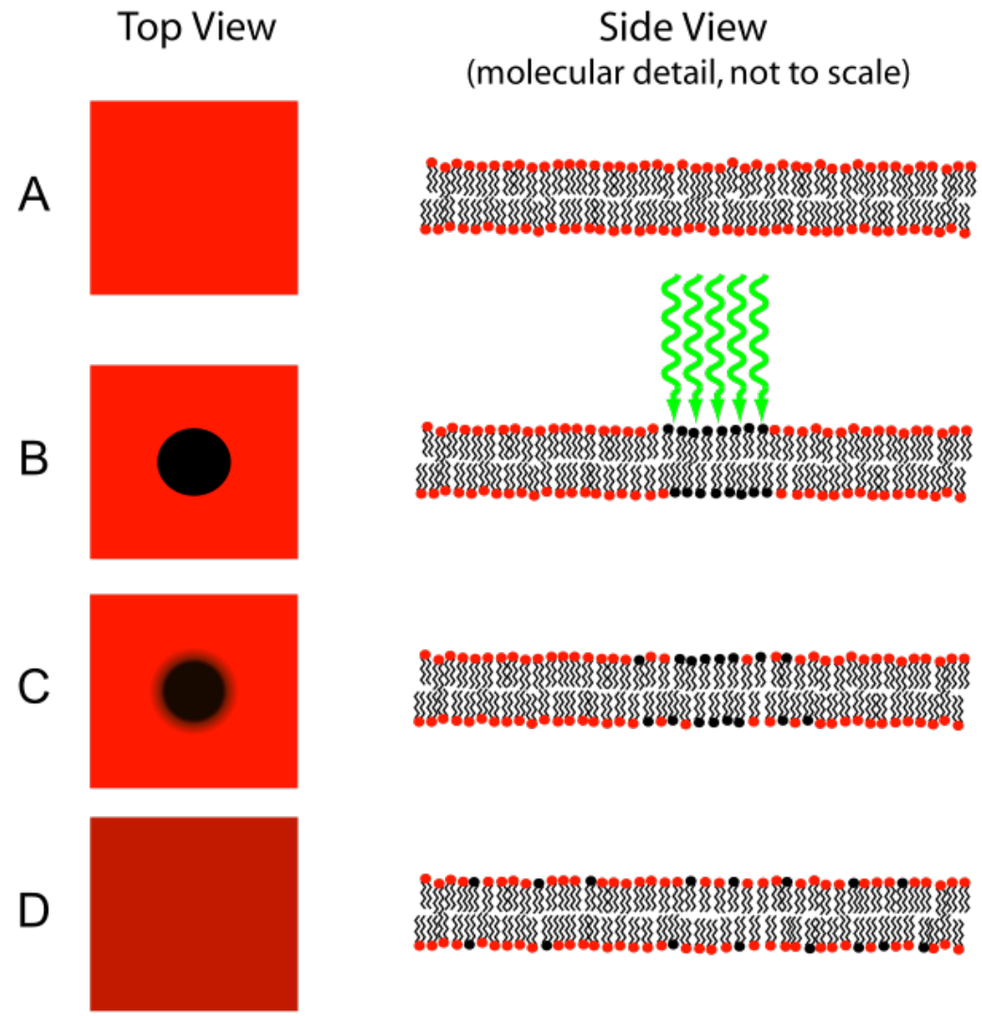

$$D = \frac{w^2}{4t_D}$$

where w is the radius of the beam and t_D is the "Characteristic" diffusion time.

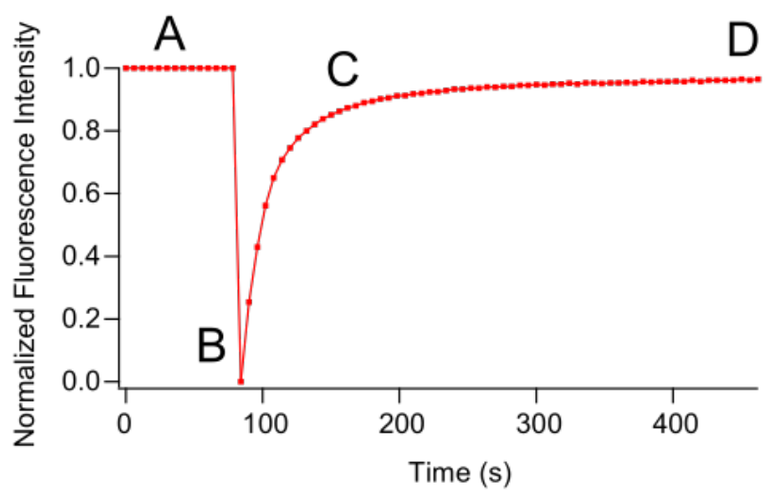

Measuring lipid diffusion - Fluorescence Correlation Spectroscopy (FCS)

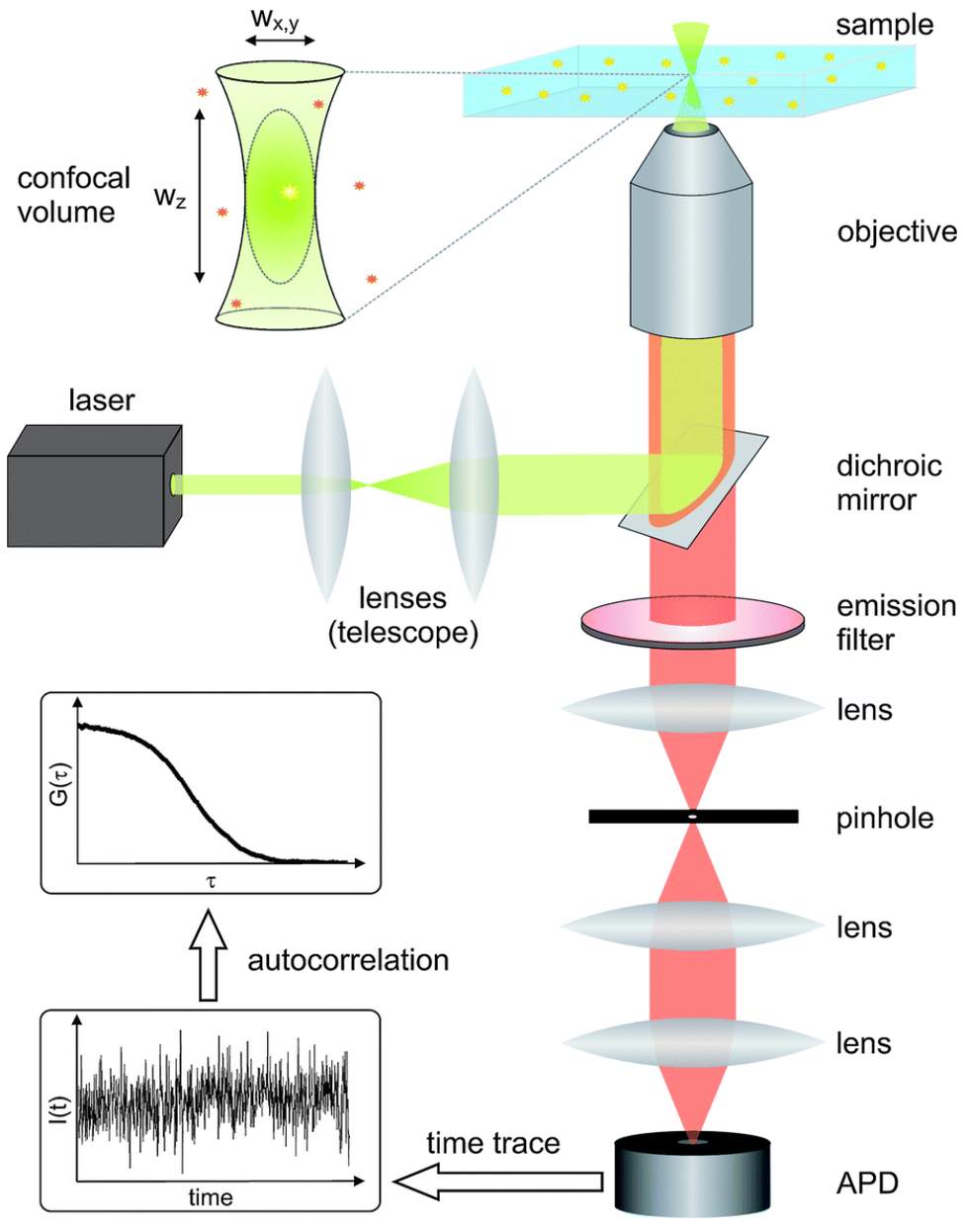

Thermodynamic Fluctuations in a Reacting System—Measurement by Fluorescence Correlation Spectroscopy

Douglas Magde,* Elliot Elson,† and W. W. Webb‡
Cornell University, Ithaca, New York 14850
(Received 10 July 1972)

The temporal correlations of thermodynamic concentration fluctuations have been measured in a chemically reactive system at equilibrium by observing fluctuations of the fluorescence of a reaction product. The experiment yields the chemical rate constants and diffusion coefficients and shows the coupling among them. Data are reported for binding of ethidium bromide to DNA.

$$G_D(\tau) = \frac{1}{N}\left(1 + \frac{\tau}{\tau_D}\right)^{-1} \qquad (2)$$

$$\tau_D = \frac{\omega^2}{4D} \qquad (3)$$

Measuring lipid diffusion - Single Particle Tracking (SPT)

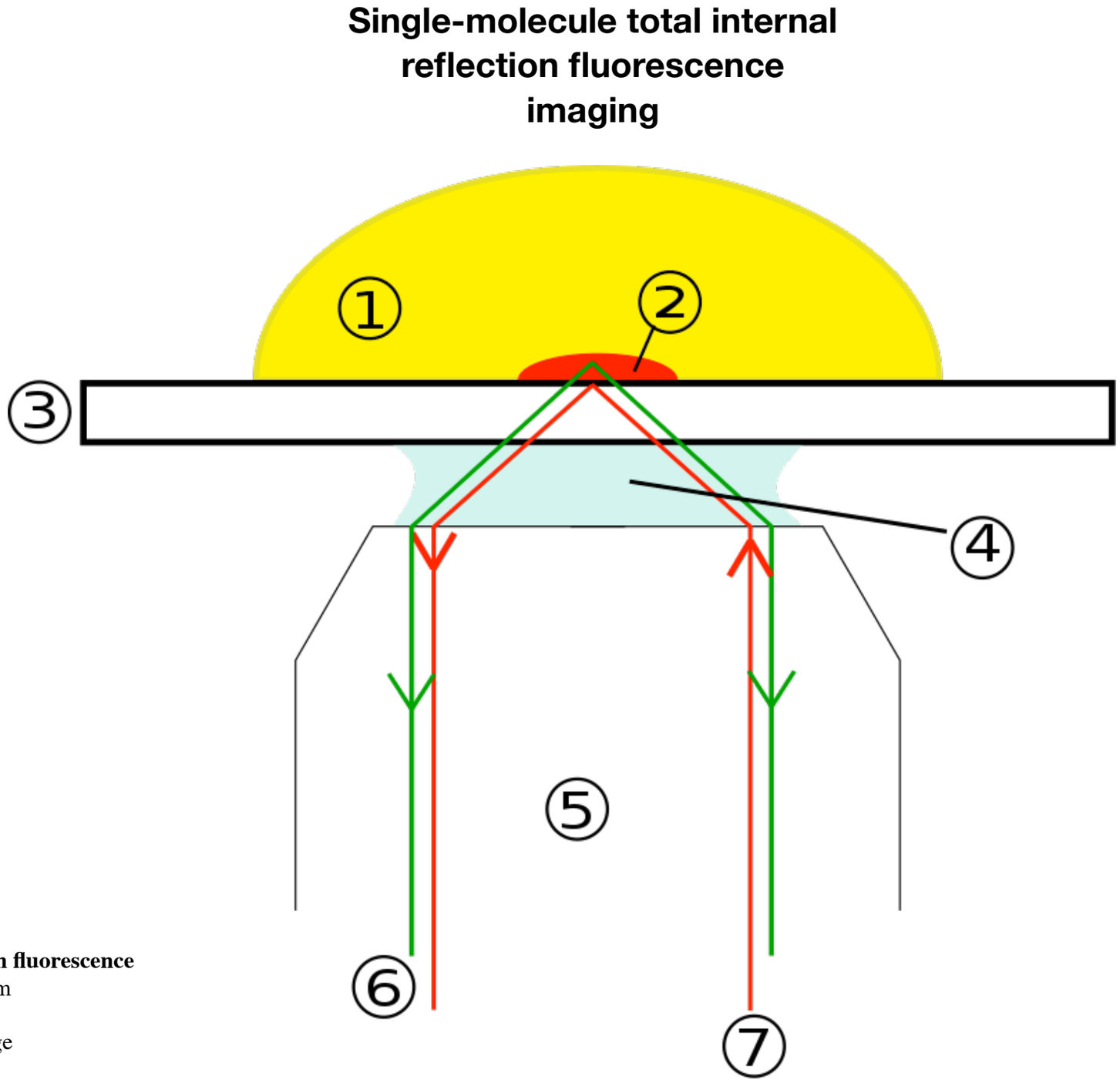

(Cis-)**total internal reflection fluorescence microscope** (TIRFM) diagram

1. Specimen
2. Evanescent wave range
3. Cover slip
4. Immersion oil
5. Objective
6. Emission beam (signal)
7. Excitation beam

Measuring lipid diffusion - Single Particle Tracking (SPT)

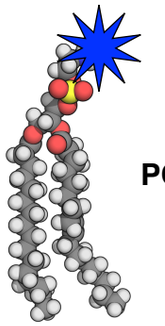

POPE-AF488
POPC
bilayer

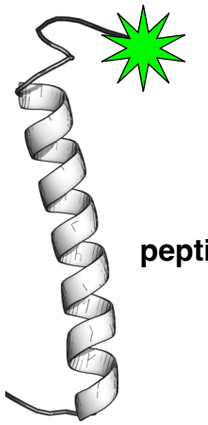

peptide-Cy3

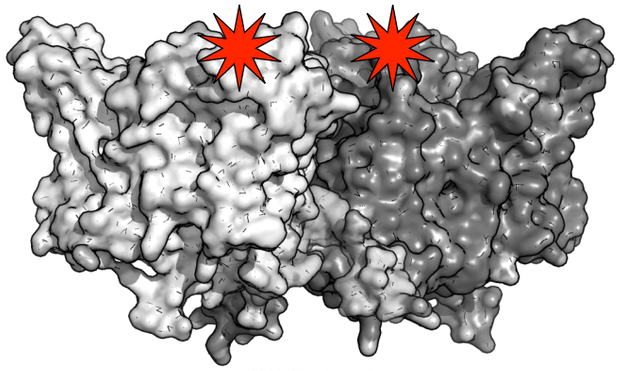

CLC-Cy5

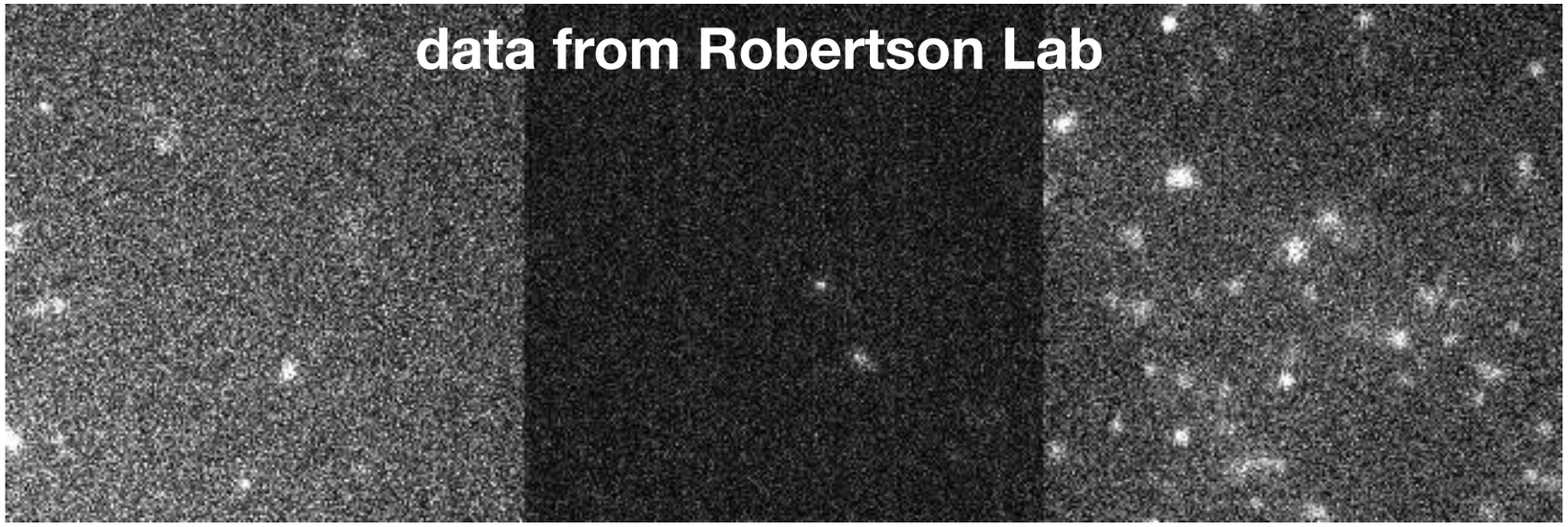

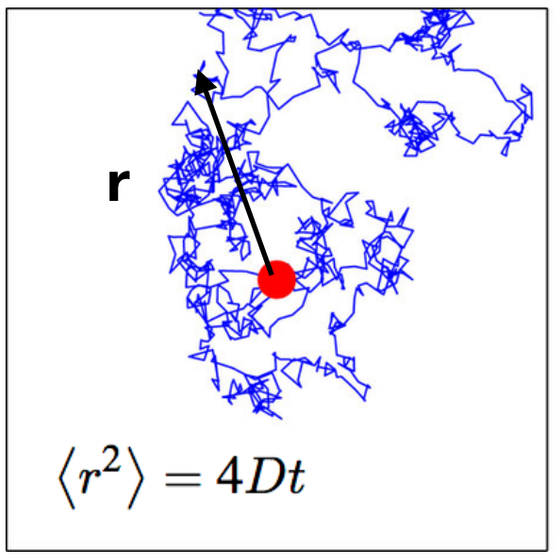

$$\mathrm{MSD} \equiv \langle |\mathbf{x}(t) - \mathbf{x_0}|^2 \rangle = \frac{1}{N} \sum_{i=1}^{N} |\mathbf{x^{(i)}}(t) - \mathbf{x^{(i)}}(0)|^2$$

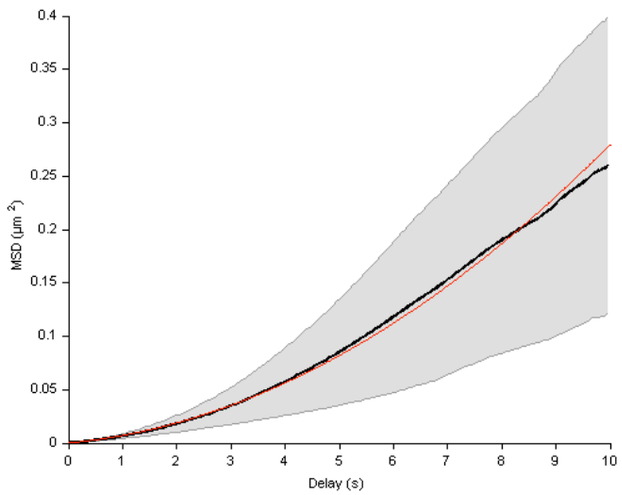

Biological Diffusion Constants

System	D ($cm^2\ s^{-1}$)	D ($\mu m^2\ s^{-1}$)
Small molecule in water	$1\text{-}1.5 \times 10^{-5}$	1000-1500
Small protein in water	10^{-6}	100
Phospholipid in membrane	10^{-8} to 10^{-7}	1-10
Protein in membrane	10^{-10} to 10^{-7}	0.01-10

Diffusion in liquid ordered phase is slower

TABLE 1

[10.1529/biophysj.105.059766]

Comparison of diffusion coefficients in the ℓ_d and ℓ_o phases for a few phospholipid/cholesterol systems

System	X_{cho}	T (°C)	Phase	D (cm^2s^{-1})	Ratio	Method	Reference
DMPC	0	35	ℓ_d	7.5×10^{-8}	–	FRAP	Rubenstein et al. (1979)
DMPC/Chol	≥0.30	35	ℓ_o	3.0×10^{-8}	2.5	–	–
DMPC	0	26	ℓ_d	6.0×10^{-8}	–	FRAP	Alecio et al. (1982)
DMPC/Chol	≥0.30	26	ℓ_o	1.8×10^{-8}	3.3	–	–
DMPC	0	35	ℓ_d	7.6×10^{-8}	–	FRAP	Vaz et al. (1985)
DMPC/Chol	≥0.30	34	ℓ_o	3.5×10^{-8}	2.2	–	Almeida et al. (1992)
DLPC	0	25	ℓ_d	3×10^{-8}	–	FCS	Korlach et al. (1999)
DLPC/Chol	0.30	25	ℓ_o	1×10^{-8}	3	–	–
DMPC	0	35	ℓ_d	11×10^{-8}	–	pfg-NMR	Filippov et al. (2003)
DMPC/Chol	0.33	35	ℓ_o	3×10^{-8}	4	–	–
SM	0	55	ℓ_d	8×10^{-8}	–	pfg-NMR	Filippov et al. (2003)
SM/Chol	0.30–0.425	55	ℓ_o	3.5×10^{-8}	2.3	–	–
DOPC	0	30	ℓ_d	10×10^{-8}	–	pfg-NMR	Filippov et al. (2003)
DOPC/Chol	0.33	30	ℓ_o(?)	5×10^{-8}	2	–	–

Biological Diffusion Constants

TABLE I. Lateral Diffusion in Lipid Bilayers

Diffusant	Molecular weight	D(cm^2/s) in fluid DMPC	Reference
Lipid analog	~1,000	(5–10) × 10^{-8}	Derzko and Jacobson [1980]
NBD-gramicidin S (cyclic)	1,150	2 × 10^{-8}	Wu et al [1978]
Glycophorin	31,000 (2,500)[a]	1–2 × 10^{-8}	Vaz et al [1982] Wu et al [1978]
Bovine rhodopsin	37,000	2 × 10^{-8}	Vaz et al [1982]
Acetylcholine receptor	~250,000	~2 × 10^{-8}	Vaz et al [1982]

[a]Molecular weight of membrane spanning portion.

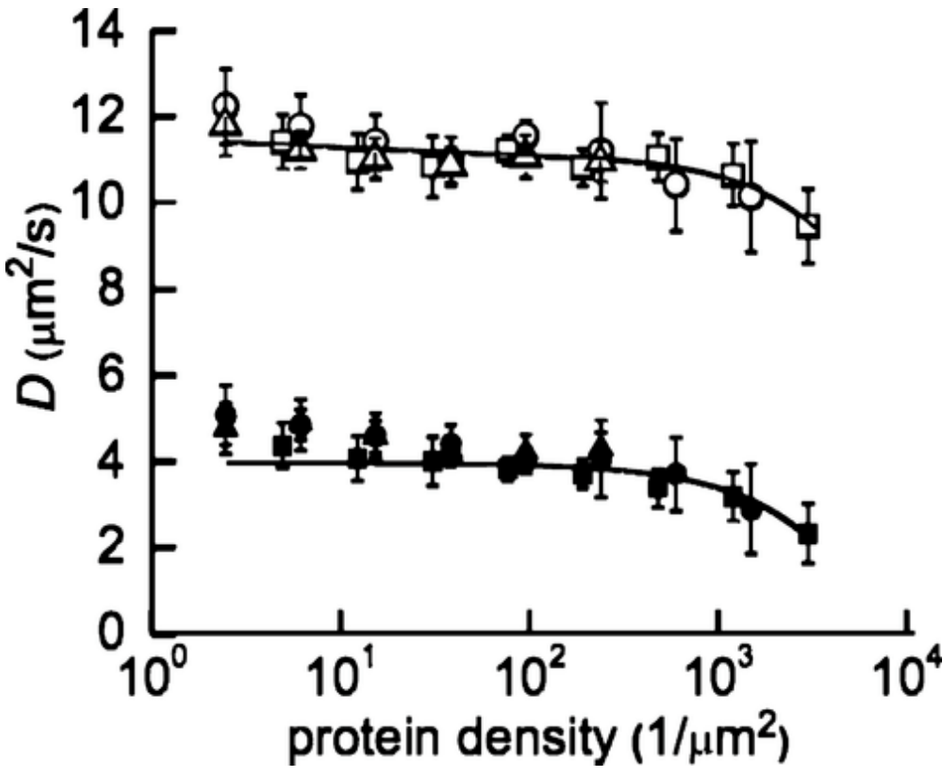

Figure 4. Lateral diffusion of protein and lipids as a function of protein density in the membrane. The labeled proteins were reconstituted in liposomes composed of DOPC/DOPG (3:1) at various protein-to-lipid ratios. The data were grouped in 9 bins logarithmically spread over the measured protein-to-lipid range. Each bin consists of at least 10 liposomes. The diffusion coefficients are shown for GltT (■) and lipids (□); LacS (●) and lipids (○); LacY (▲) and lipids (Δ). The solid lines are linear fits for GltT (■, □).

Ramadurai S, Duurkens R, Krasnikov VV, Poolman B. Lateral diffusion of membrane proteins: consequences of hydrophobic mismatch and lipid composition. Biophys J. 2010 Sep 8;99(5):1482-9. doi: 10.1016/j.bpj.2010.06.036. PMID: 20816060; PMCID: PMC2931744.

Diffusion in 2D vs. 3D

In 3D viscous liquid:

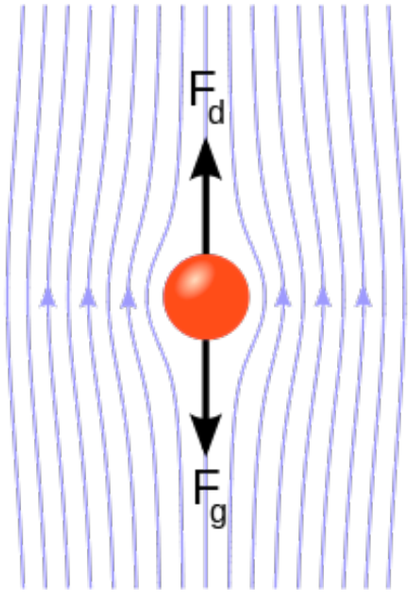

Stokes-Einstein equation

$$D = \frac{k_B T}{6\pi\mu R_0}$$

D – diffusion coefficient
μ- solvent viscosity
R_0 – solute radius
k_B – Boltzmann's constant
T – temperature (K)

In 2D viscous liquid:

Stokes paradox - no creeping flow around a disk in 2D

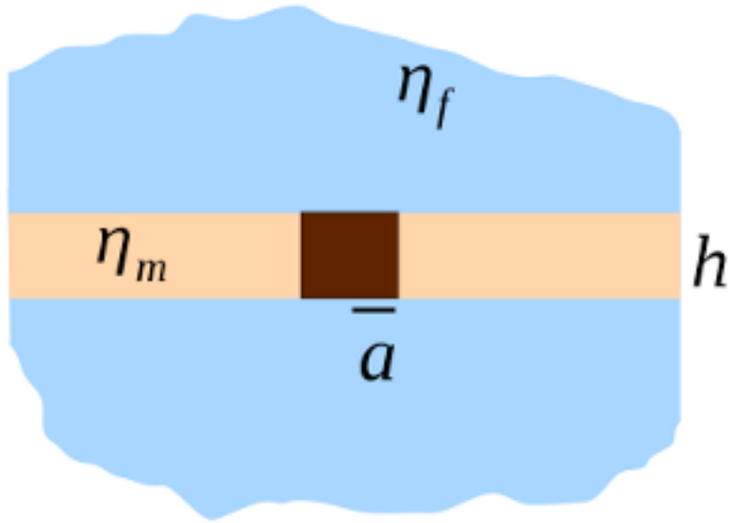

Saffman and Delbrück continuum hydrodynamic model for 2D

$$D = \frac{k_B T}{4\pi\mu h}\left(\ln\left(\frac{\mu h}{\mu' R}\right) - \gamma\right)$$

h - membrane thickness
μ - viscosity
r - radius
γ - Euler-Mascharoni constant ≈ 0.577
μ' - bulk fluid viscosity

Membrane protein diffusion follows Saffran-Delbruck model

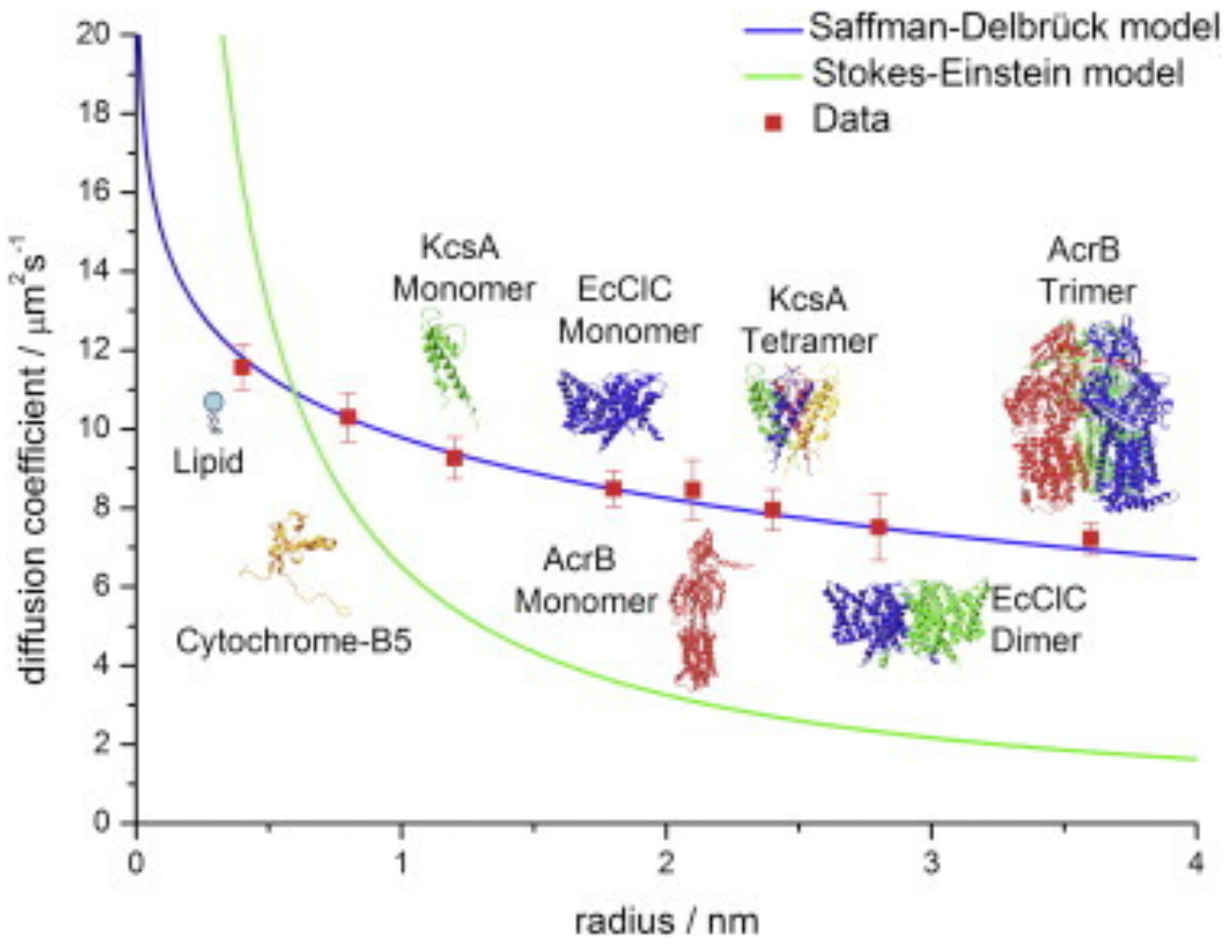

Weiß K, Neef A, Van Q, Kramer S, Gregor I, Enderlein J. Quantifying the diffusion of membrane proteins and peptides in black lipid membranes with 2-focus fluorescence correlation spectroscopy. *Biophys J*. 2013;105(2):455-462. doi:10.1016/j.bpj.2013.06.004

Diffusion is slower in cellular membranes

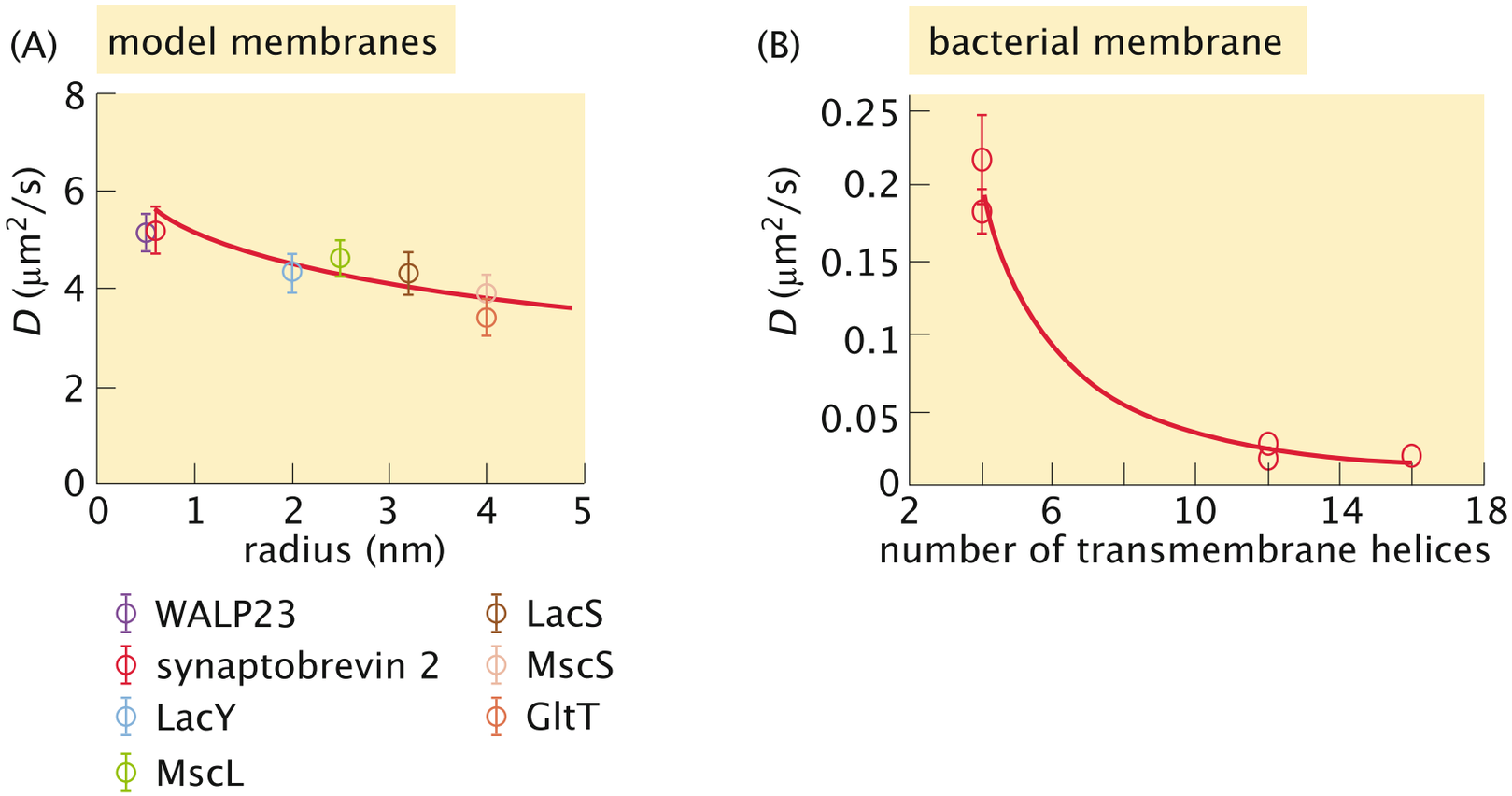

Fig. 12 Range of diffusion coefficients. (**a**) Diffusion coefficients for different membrane proteins measured using fluorescence correlation spectroscopy in giant unilamellar vesicles showing dependence on protein size. The red line is a fit using the Saffman-Delbrück model which characterizes membrane diffusion as a function of the size of the diffusing molecule [52, 53]. (**b**) Diffusion coefficients for different membrane proteins measured using fluorescence recovery after photobleaching (FRAP) in the *E. coli* cell membrane. The red line is an empirical fit as a function of the number of transmembrane helices in the protein. The names refer to particular membrane proteins used in the experiments. (**a**) adapted from [54] and (**b**) adapted from [55]

Diffusion in cellular membranes demonstrates distinct behaviors

Tomishige et al., 1998. DOI: 10.1083/jcb.142.4.989

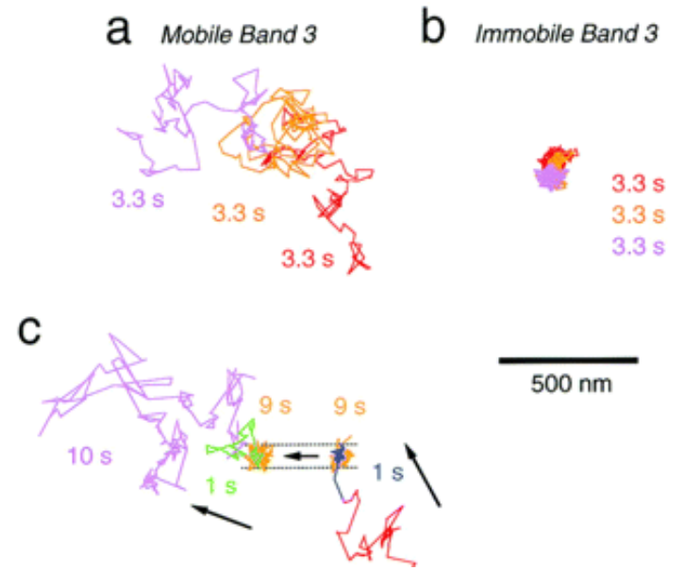

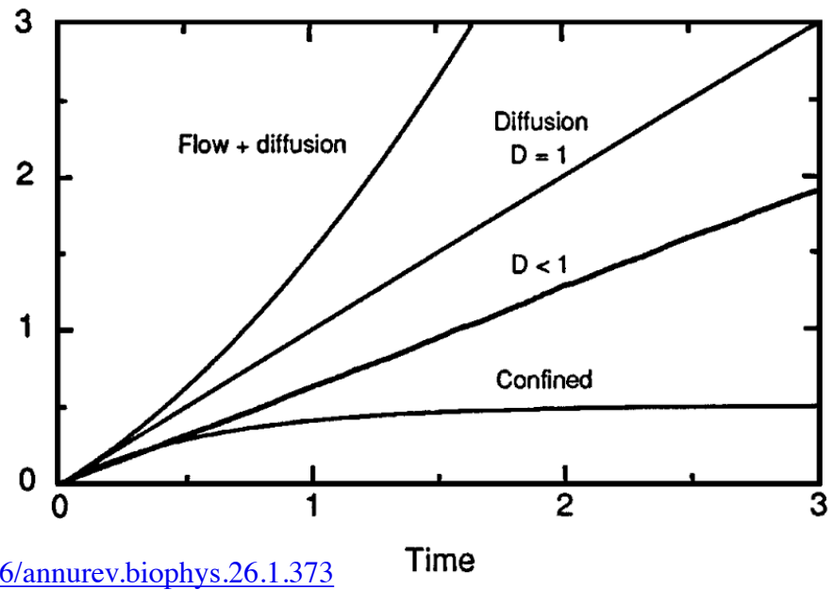

DOI: 10.1146/annurev.biophys.26.1.373

Figure 1 The mean-square displacement $\langle r^2 \rangle$ as a function of time t for simultaneous diffusion and flow, pure diffusion, diffusion in the presence of obstacles, and confined motion.

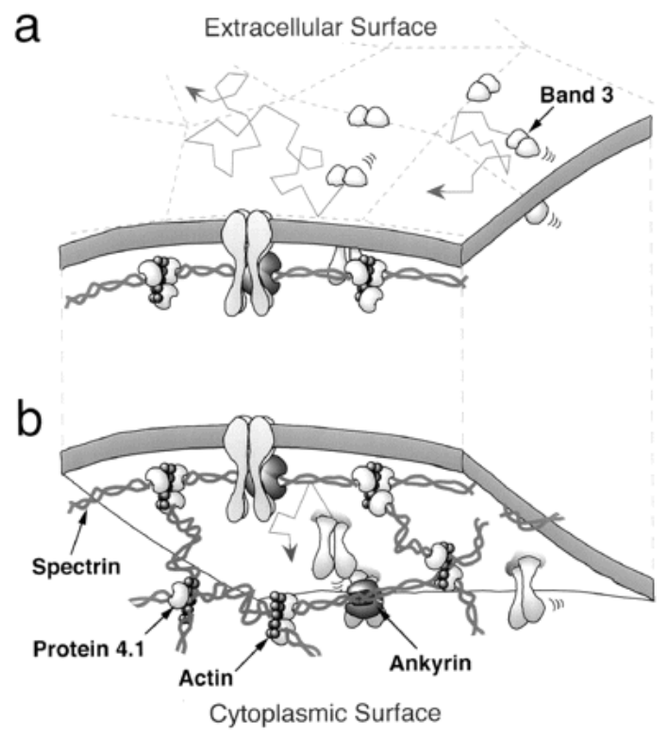

1. **Stationary mode - D < 4.6 x 10^{-12} cm^2/s (6%)**
2. **Simple Brownian diffusion mode (28%)**
3. **Directed diffusion with unidirectional motion (2%)**
4. **Confined diffusion within domains with Brownian diffusion between D = 4.6 x 10^{-12} cm^2/s and 10^{-9} cm^2/s (64%).**

Lipid flip flop (transverse movement)

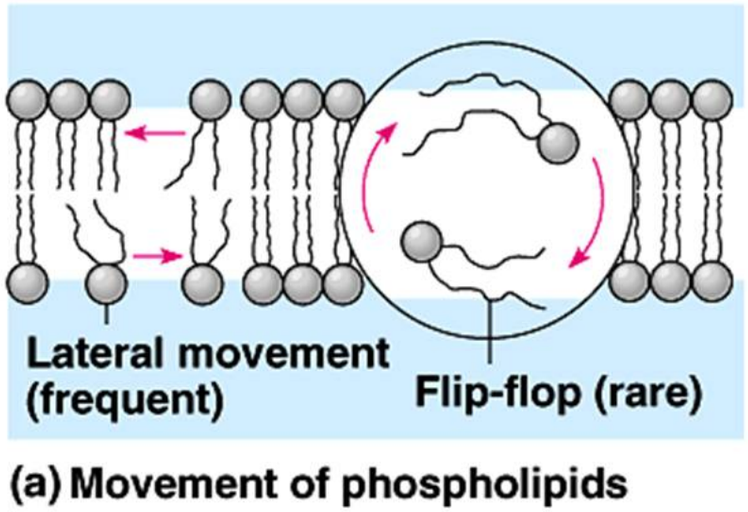

(a) Movement of phospholipids

Kornberg & McConnell 1971

DOI: 10.1021/bi00783a003

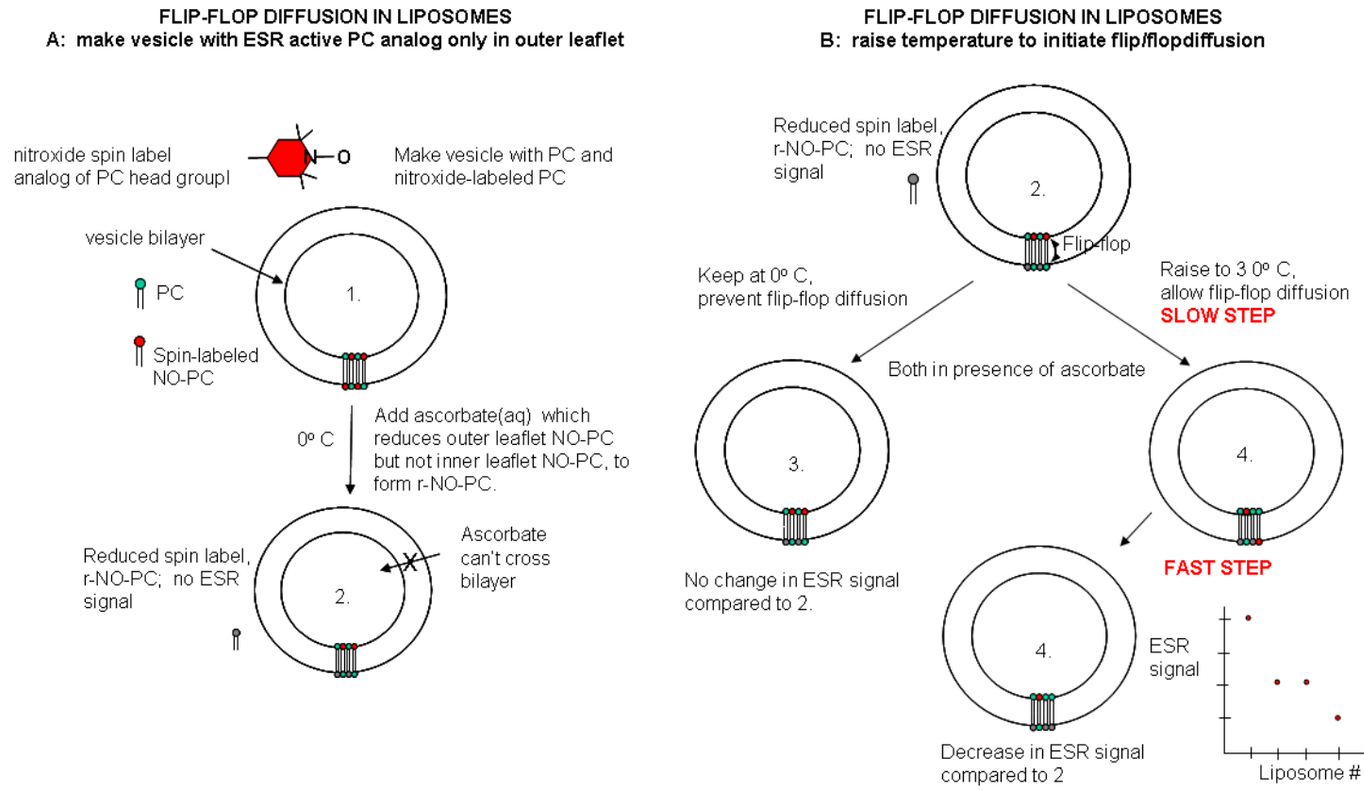

Rate of flip flop is 0.00002/sec

Translation step for lateral diffusion is 3000/sec

Molecular dynamics simulations of membranes

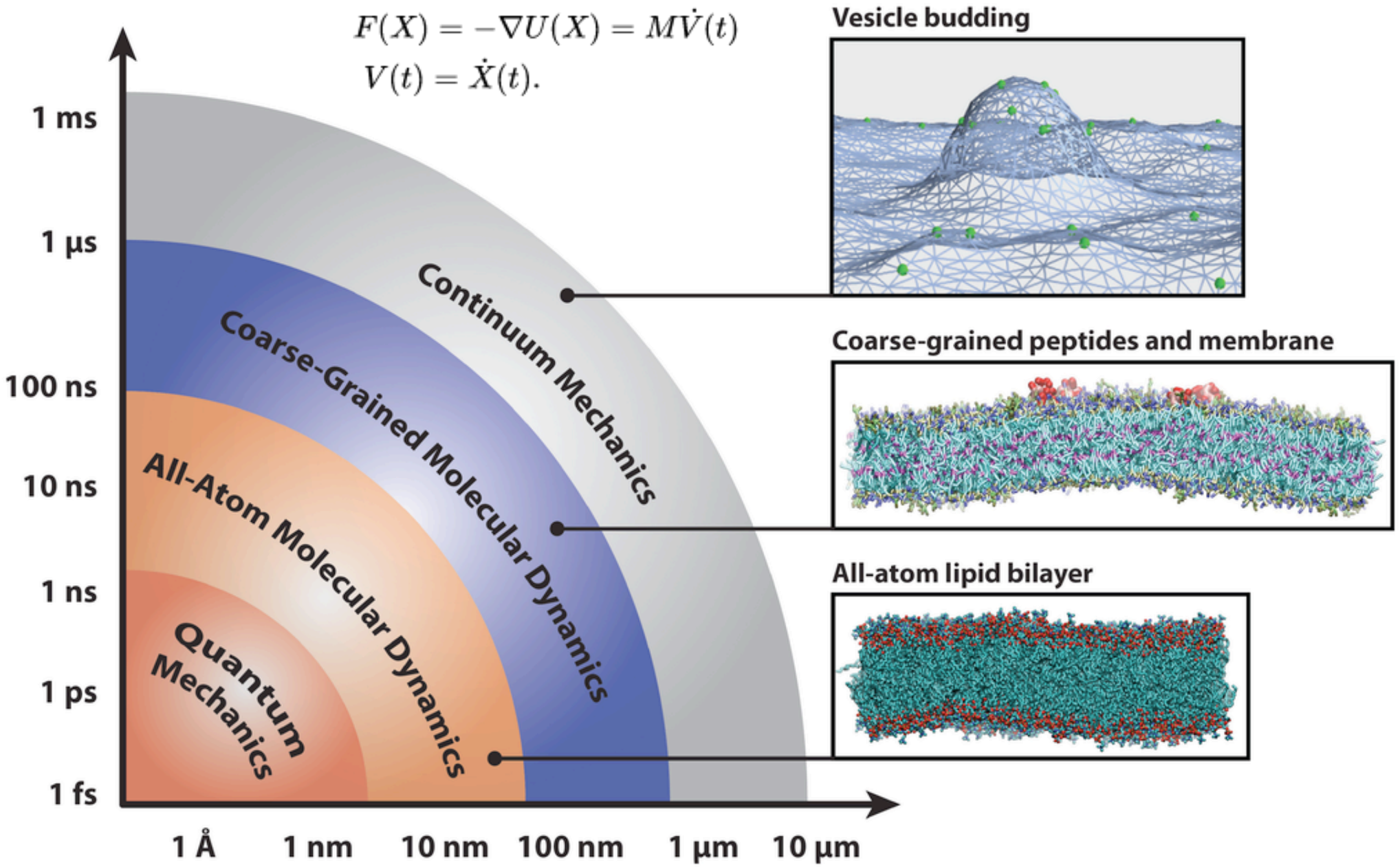

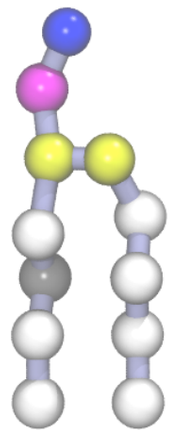

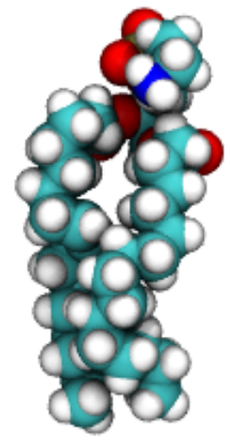

Figure 1. Diagram of computational methods for studying biophysical systems across a range of time- and length-scales. Representative snapshots depict an all-atom lipid bilayer, peptides embedded in a coarse-grained bilayer and proteins remodeling a continuum mechanics membrane model. Bilayers were simulated with the CHARMM36 [15] and Martini [16] force fields and rendered with Visual Molecular Dynamics [17].

Bradley & Rhadakrishnan, *Polymers* **2013**, *5*(3), 890-936; https://doi.org/10.3390/polym5030890

Molecular dynamics simulations of membranes

<u>Simulation details</u>
Software: Gromacs
FF: MARTINI
Simulation time: 160 μs total
10 + 8 replicas

<u>Lipid composition</u>
headgroup: 67% PE, 33% PG
tails: 100% PO

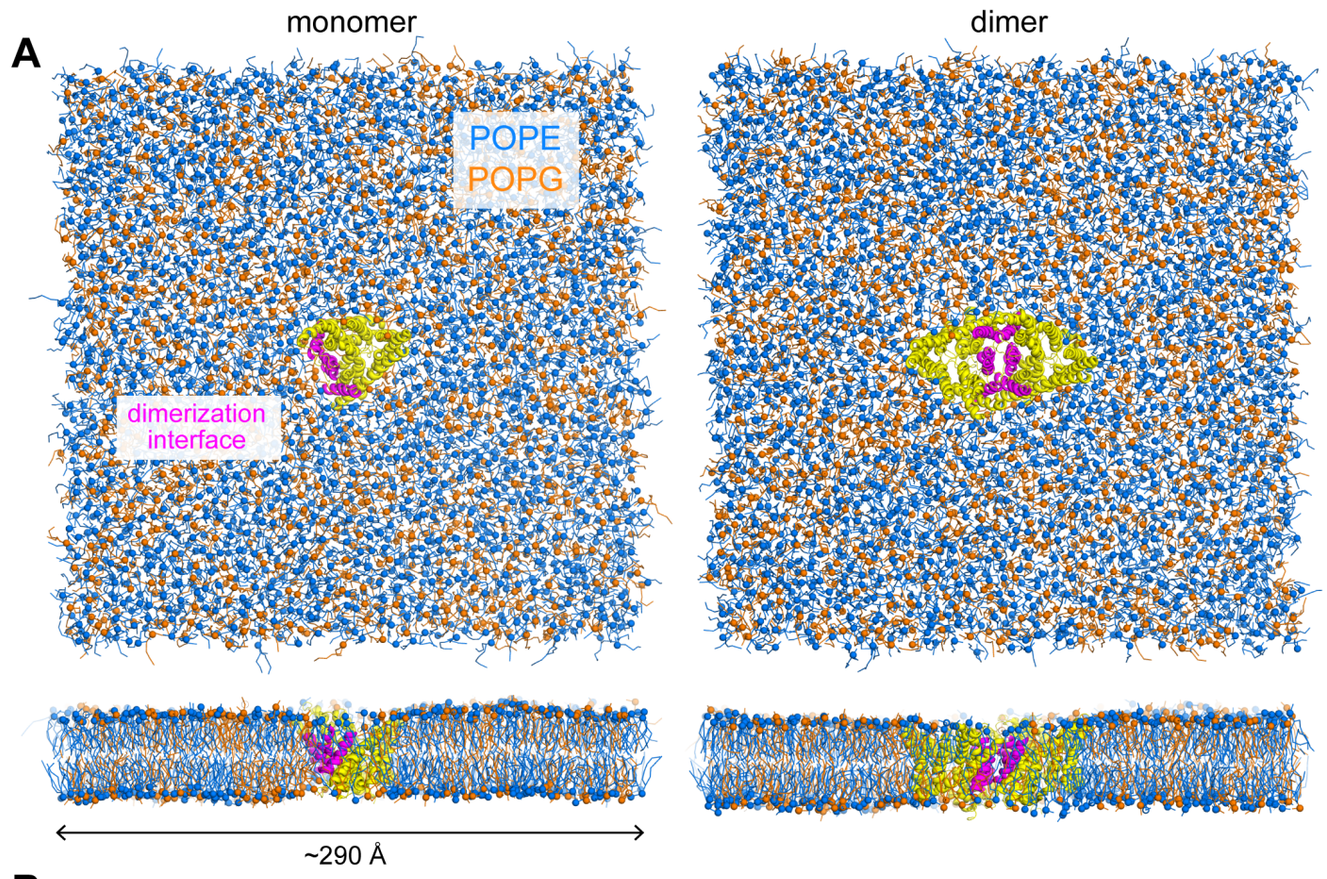

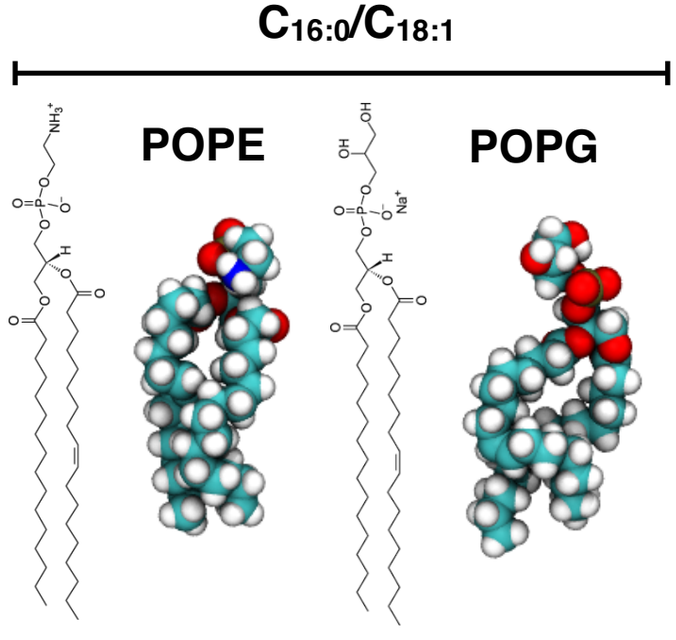

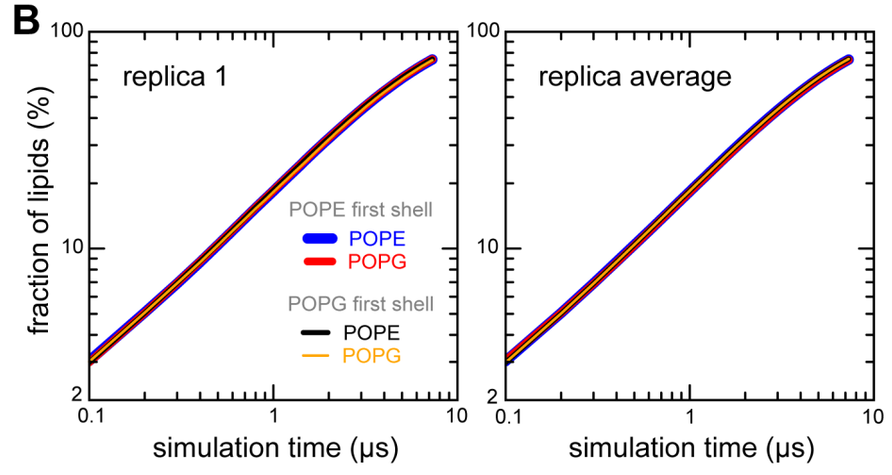

Chadda, Bernhardt, Kelley, Teixeira, Griffith, Gil-Ley, Ozturk, Hughes, Forsythe, Krishnamani, Faraldo-Gómez* & Robertson*, eLife 2021

Molecular dynamics simulations of membranes

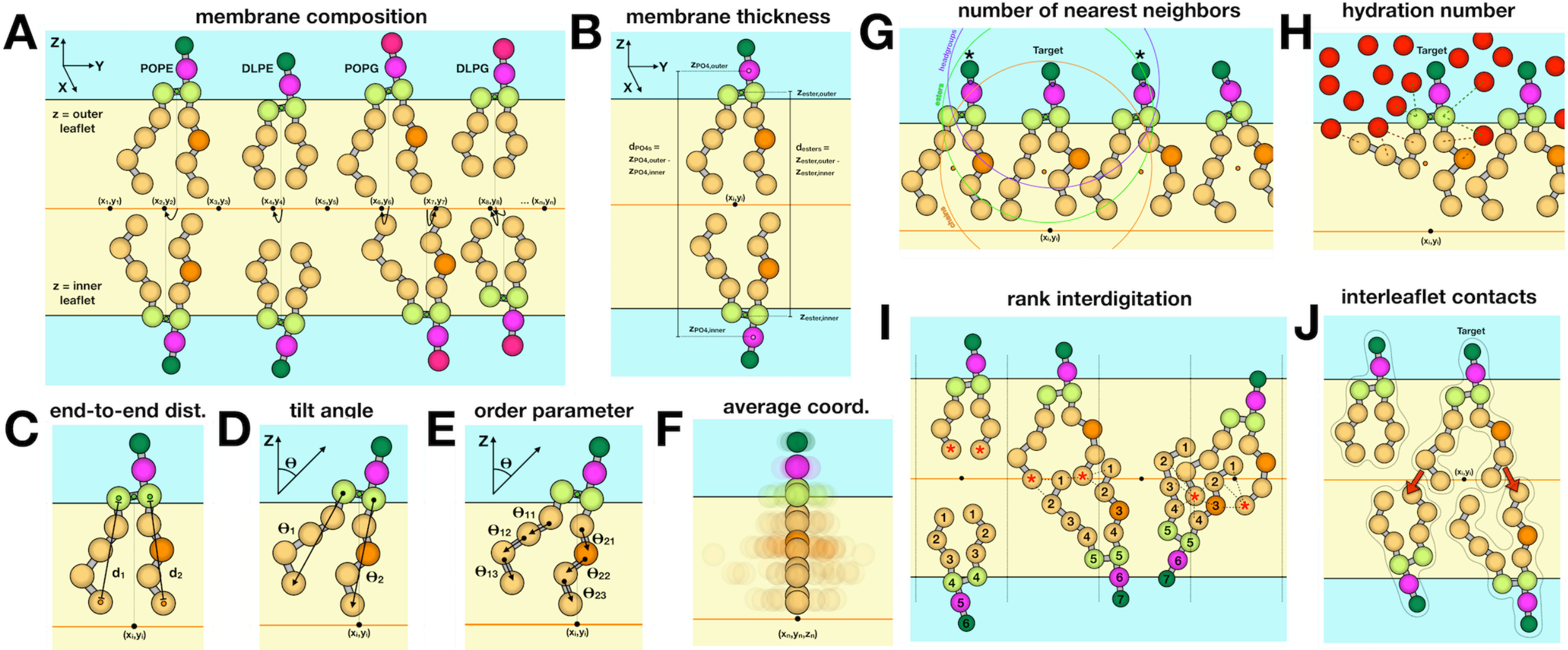

Molecular dynamics simulations of membranes

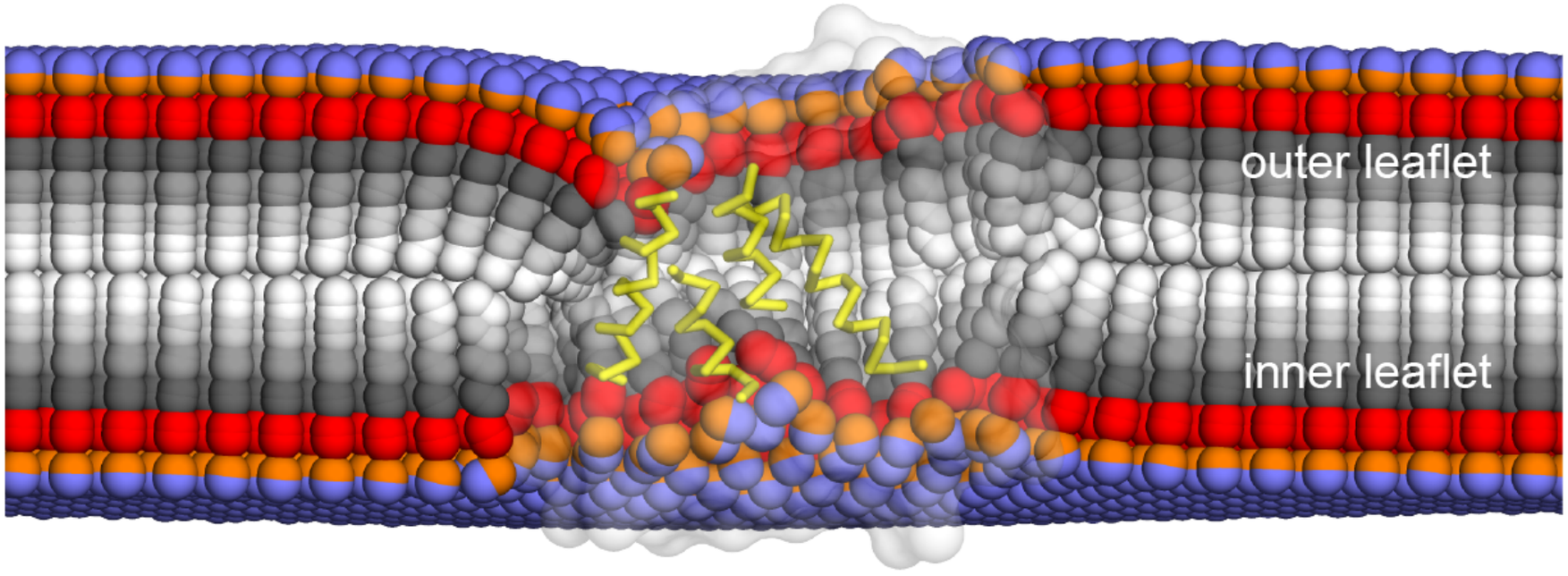

time-averaged lipid structures

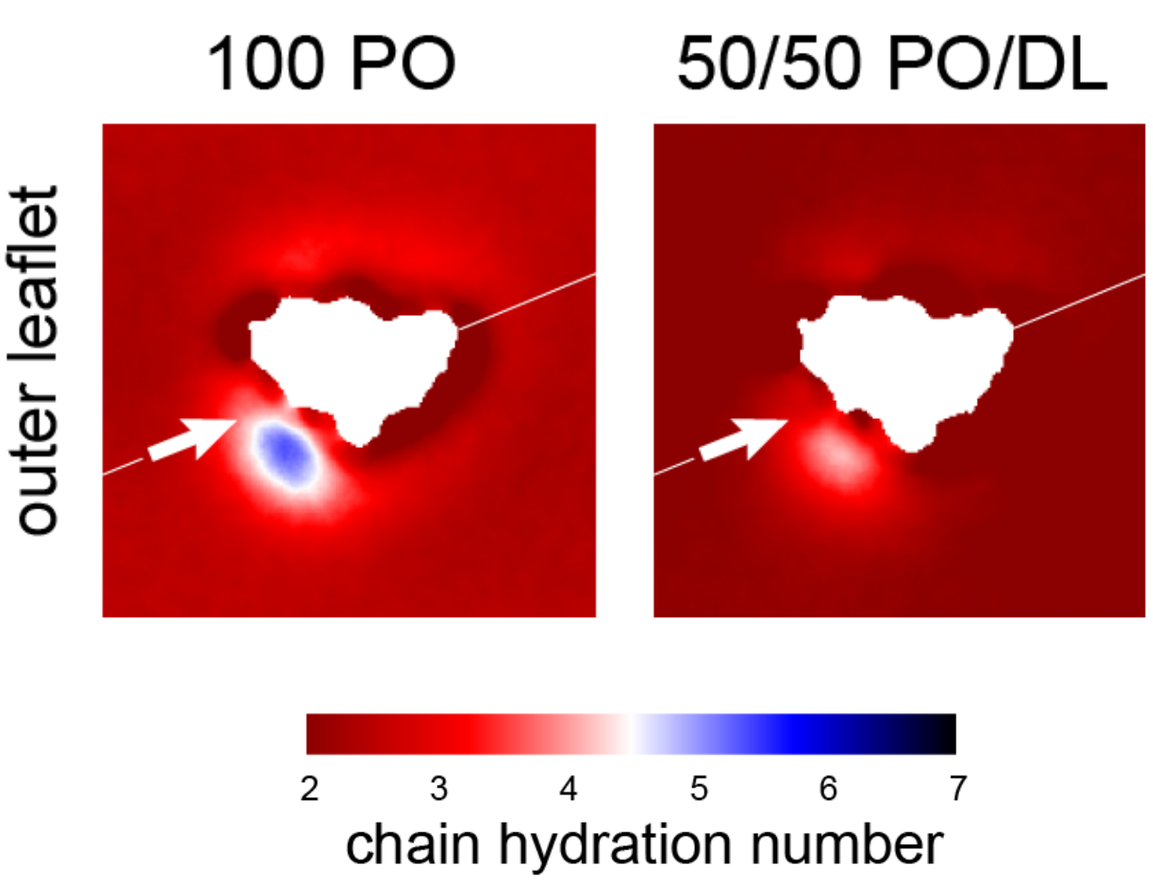

Molecular dynamics simulations of membranes

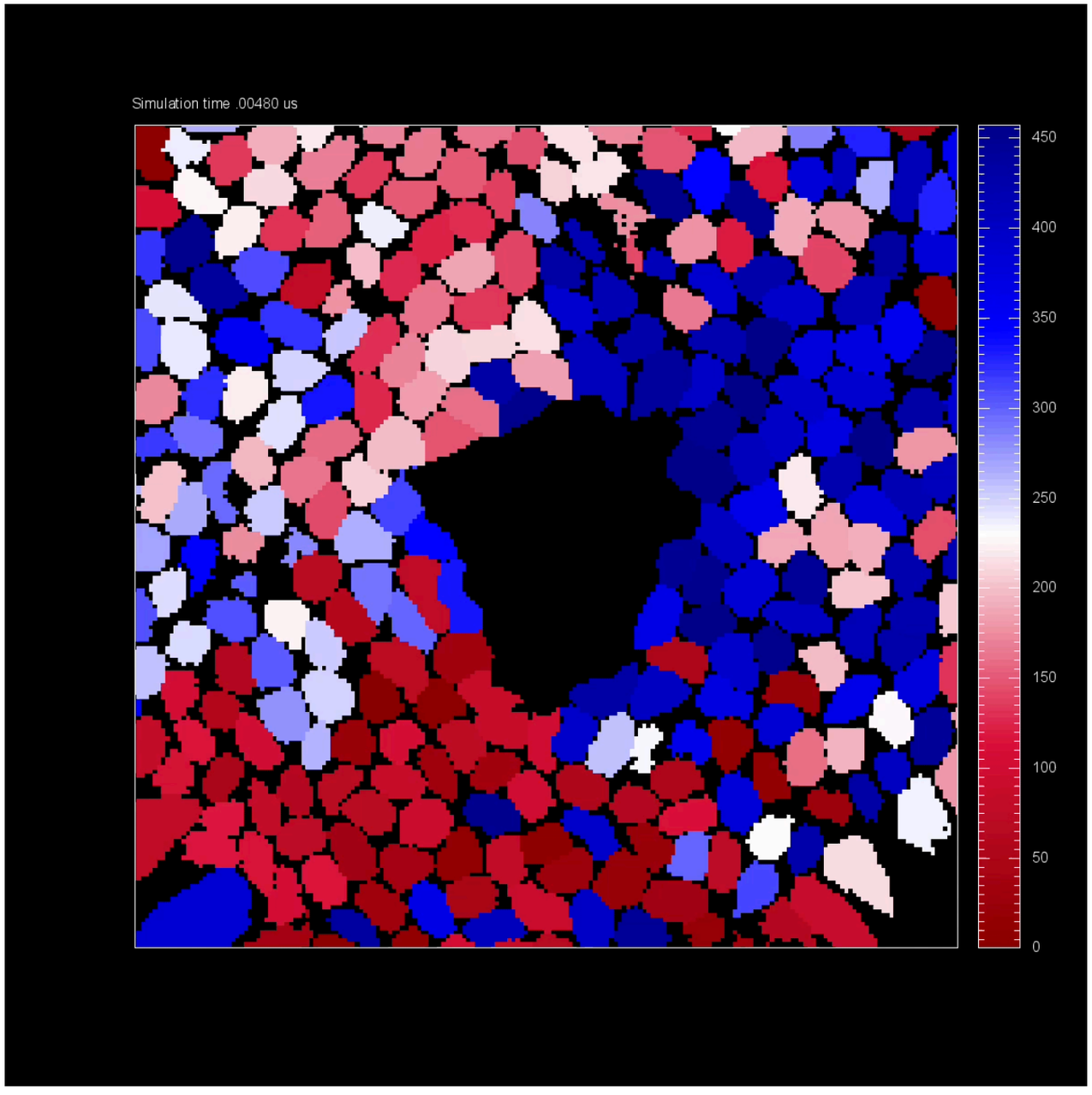

Molecular dynamics simulations of membranes

- Mechanics & dynamics

Table 1. Descriptors of membrane structure and dynamics accessible in MOSAICS 1.0 and in other simulation analysis tools[‡]

	MOSAICS	LiPyphilic	LoMePro	APL*Voro	LipidDyn	Grid-MAT	LOOS	Membrainy	MEMB-PLUGIN	MemSurfer
Bilayer shape	Yes	Yes	----	----	----	----	Yes	----	----	Yes
Bilayer thickness	Yes	Yes	Yes	Yes	----	Yes	----	Yes	Yes	Yes
Lipid-chain order parameter*	Yes	Yes	Yes	----	----	----	Yes	----	----	----
Area per lipid*	Yes	Yes	Yes	Yes	----	----	----	----	----	Yes
Multicomponent lipid enrichment*	Yes	----	----	----	Yes	----	----	----	----	----
Lipid density*	Yes	----	----	----	Yes	----	Yes	Yes	Yes	Yes
Mean lipid tilt*,§	Yes	----	----	----	----	----	Yes	----	----	----
Mean instantaneous lipid tilt*,§	Yes	Yes	----	----	----	----	----	----	----	----
Leaflet interdigitation	Yes	----	----	----	----	----	----	----	----	----
Interleaflet contacts*	Yes	----	----	----	----	----	----	----	----	----
Lipid-chain end-to-end length*	Yes	----	----	----	----	----	----	----	----	----
Lipid-chain splay*	Yes	----	----	----	----	----	----	----	----	----
Lipid-solvent contacts*	Yes	----	----	----	----	----	----	----	----	----
Lipid-protein H-bond & salt-bridges	Yes	----	----	----	----	----	----	----	----	----
Average lipid conformation*	Yes	----	----	----	----	----	----	----	----	----
Lipid radius of gyration	Yes	----	----	----	----	----	----	----	----	----
Lipid residence time	Yes	----	----	----	----	----	----	----	----	----
Multicomponent lipid mixing	Yes	----	----	----	----	----	----	Yes	----	----
Lipid self-diffusion coefficients	Yes	Yes	----	----	----	----	----	----	----	----
Lipid solvation-shell on/off rates	Yes	----	----	----	----	----	----	Yes	----	----
Lipid flipping	Yes	Yes	----	----	----	----	----	----	----	----
Membrane protein tilt angle	Yes	----	----	----	----	----	----	----	----	----
Parallelization	MPI	----	----	----	Multi-core	----	Multi-core	Multi-core	----	----
Supported trajectory file format	GROMACS	Multiple	GROMACS	GROMACS	GROMACS	GROMACS	Multiple	GROMACS	Multiple	Multiple
Programming language	C++	Python	C	C++	Python	Perl	C++	Java	TCL	C++/Python

([‡]) In MOSAICS 1.0, most descriptors are provided as 2D spatial distributions across the membrane plane, which can be represented as heat maps filtered by user-defined statistical-significance thresholds; selected observables (*) are also available as 3D distributions. Only self-diffusion coefficients and lipid-mixing are provided as global average properties. Descriptors available in other software tools but not in MOSAICS 1.0 are not included in this table, for conciseness; we refer the reader to the corresponding publications for further details. ([§]) Further details on these alternative definitions are provided below.

Bernhardt N, Faraldo-Gómez JD. MOSAICS: A software suite for analysis of membrane structure and dynamics in simulated trajectories. Biophys J. 2022 Nov 3:S0006-3495(22)00903-1. doi: 10.1016/j.bpj.2022.11.005. Epub ahead of print. PMID: 36333911.

Molecular dynamics simulations of membranes

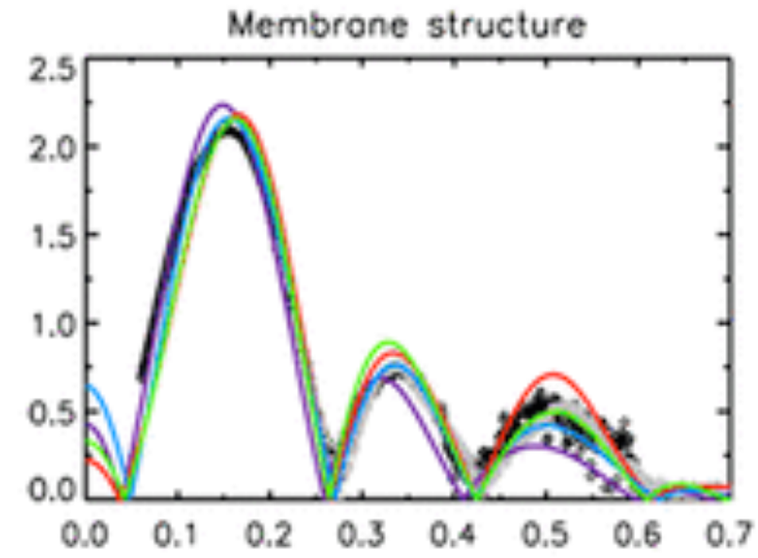

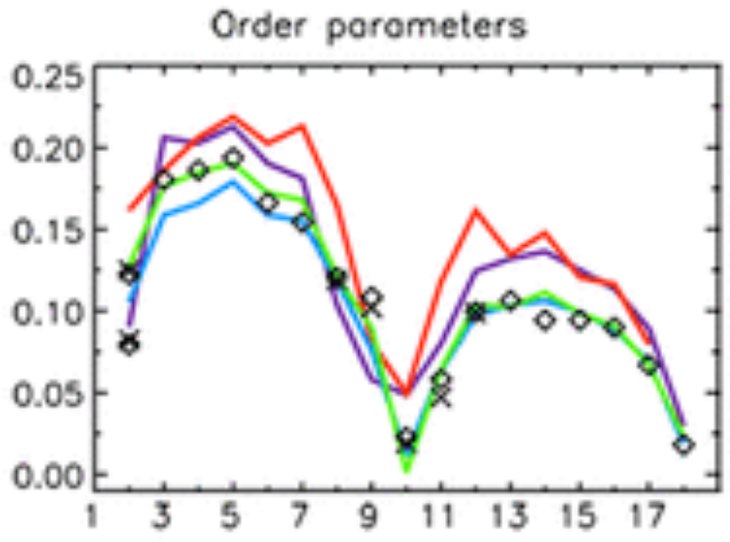

Slipids

Lipid14

?

CHARMM36

GROMOS54a7

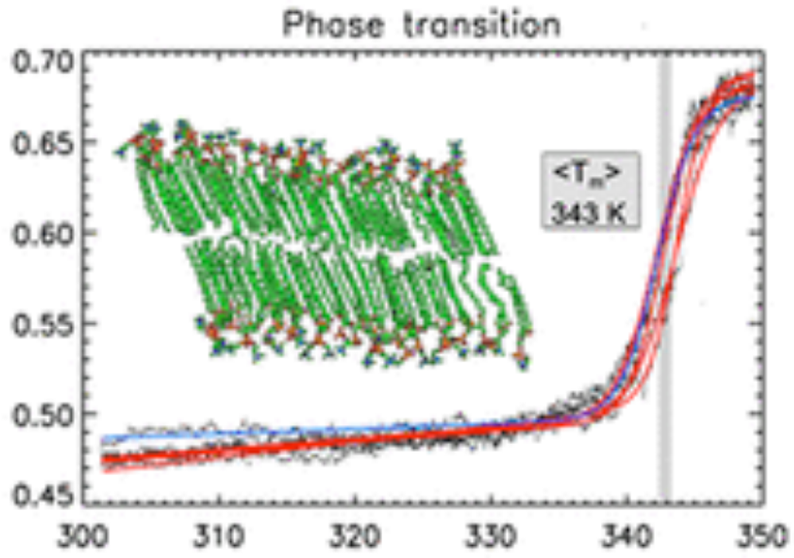

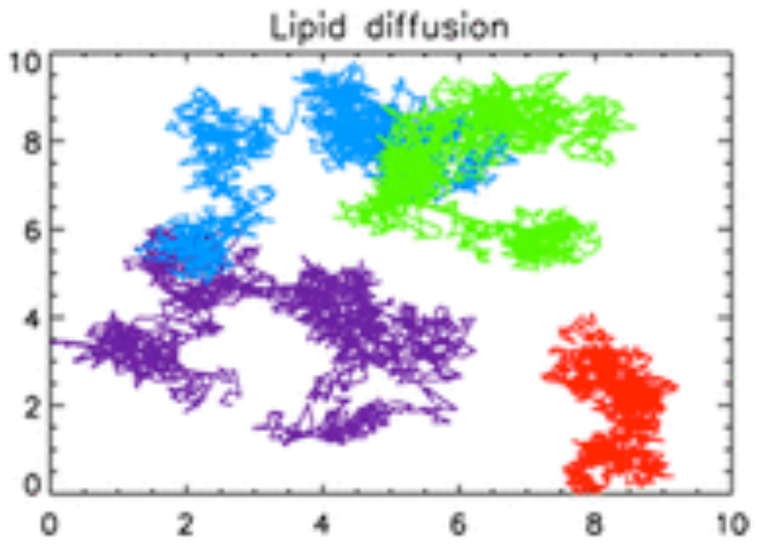

Leonard et al., *Chem. Rev.* 2019, 119, 9, 6227–6269
https://doi.org/10.1021/acs.chemrev.8b00384

Table 2 Membranes by the numbers

Membrane parameter	Range of parameter values	BNID
Lipid length	≈2.5–3.5 nm	See Table 1
Lipid area	≈1/4–3/4 nm^2	See Table 1
Number of lipids per cell (bacterium)	$\approx 2 \times 10^7$	100071
Bending rigidity	10–25 $k_B T$	105297
Area stretch modulus	200–250 mN/m (or ≈50 $k_B T/nm^2$)	112590, 112659
Membrane tension	$10^{-4} - 1\, k_B T/nm^2$	110849,112509, 112519
Rupture tension	1–2 $k_B T/nm^2$	112489, 110911
Membrane permeability (water)	10–50 μm/s	112488
Membrane capacitance	≈1 $\mu F/cm^2$	110759, 109244, 110802
Membrane resistance	0.1–1.5 $\times 10^9\ \Omega\, cm^2$	110802
Membrane potential	100 mV	109775, 107759
Diffusion constant (lipid)	≈1 $\mu m^2/s$	112471, 112472
Diffusion constant (membrane protein)	≈0.02–0.2 $\mu m^2/s$	107986

A summary of the key numbers about membranes discussed throughout the chapter for easy reference. Numbers reported are "typical" values and should be used as a rule of thumb. For a more detailed description of parameter values, the reader should use the Bionumbers database through the relevant BNID. Also see Box 1 of [14]

Phillips 2018